Posted on 30 Aug 2023 — The copyright holder is the author/funder. All rights reserved. No reuse without permission. — https://doi.org/10.22541/au.169339743.30080820/v1 — This a preprint and has not been peer reviewed. Data may be preliminary.

How mantis shrimp compound eye recognizes circularly polarized light

Fangrui Lou[1], Xiuyu Qu[2], Celia Schunter[3], Lin Wang[4], Yongzheng Tang[2], Zhiqiang Han[2], and Bin Kang[5]

[1]Yantai University
[2]Affiliation not available
[3]University of Hong Kong School of Biological Sciences
[4]CAS Key Laboratory of Experimental Marine Biology, Institute of Oceanology, Chinese Academy of Sciences
[5]Ocean University of China

August 30, 2023

Abstract

The mantis shrimps are the only animal species known to science that can recognize circularly polarized light (CPL). Here we explored the morphological and molecular mechanisms of CPL recognition in *Oratosquilla oratoria*, a typical species of mantis shrimps. Through multilayer microscopy, we discovered the cross-arranged microvilli and the oval distal rhabdom to be the critical structures for CPL recognition. Based on the specific expression patterns of vision-related functional genes and proteins, we suggest that the order of light utilization by *O. oratoria* compound eye was first natural light, then left-rotation CPL (LCPL), linearly polarized light, right-rotation CPL (RCPL) and dark. Meanwhile, we found that the expression levels of vision-related functional genes and proteins in *O. oratoria* compound eye under RCPL were not significantly different from those in DL, and thus provide additional evidence that mantis shrimp can only recognize LCPL. Furthermore, the recognition of LCPL is likely facilitated by the differential expression of opsin and microvilli - related functional genes and proteins (arrestin and sodium-coupled neutral amino acid transporter). In conclusion, this study systematically illustrated for the first time how *O. oratoria* compound eye recognizes CPL, and it can improve the visual ecological theory behind polarized light recognition.

How mantis shrimp compound eye recognizes circularly polarized light

Lou Fangrui[1], Qu Xiuyu[1], Celia Schunter[2], Wang Lin[3], Tang Yongzheng[1], Han Zhiqiang[4*], Kang Bin[5*]

1 School of Ocean, Yantai University, Yantai, Shandong, 264005, China

2 Swire Institute of Marine Science, School of Biological Sciences, The University of Hong Kong Hong Kong SAR, China

3 Key Laboratory of Sustainable Development of Marine Fisheries, Ministry of Agriculture and Rural Affairs, Yellow Sea Fisheries Research Institute, Chinese Academy of Fishery Sciences, Qingdao, Shandong, 266071, China

4 Fishery College, Zhejiang Ocean University, Zhoushan, Zhejiang, 316022, China

5 Fisheries College, Ocean University of China, Qingdao, Shandong, 266003, China

*Corresponding author: Zhiqiang Han, Fishery College, Zhejiang Ocean University, Zhoushan, Zhejiang, 316022, China, Email:*d6339124@163.com*; Bin Kang, Fisheries College, Ocean University of China, Qingdao,

Shandong, 266003, China, Email: *binkang@163.com*.

Abstract : The mantis shrimps are the only animal species known to science that can recognize circularly polarized light (CPL). Here we explored the morphological and molecular mechanisms of CPL recognition in*Oratosquilla oratoria,* a typical species of mantis shrimps. Through multilayer microscopy, we discovered the cross-arranged microvilli and the oval distal rhabdom to be the critical structures for CPL recognition. Based on the specific expression patterns of vision-related functional genes and proteins, we suggest that the order of light utilization by *O. oratoria* compound eye was first natural light, then left-rotation CPL (LCPL), linearly polarized light, right-rotation CPL (RCPL) and dark. Meanwhile, we found that the expression levels of vision-related functional genes and proteins in*O. oratoria* compound eye under RCPL were not significantly different from those in DL, and thus provide additional evidence that mantis shrimp can only recognize LCPL. Furthermore, the recognition of LCPL is likely facilitated by the differential expression of opsin and microvilli - related functional genes and proteins (arrestin and sodium-coupled neutral amino acid transporter). In conclusion, this study systematically illustrated for the first time how *O. oratoria*compound eye recognizes CPL, and it can improve the visual ecological theory behind polarized light recognition.

Key words :*Oratosquilla oratoria* ; rhabdom; microvilli; opsin; visual ecology.

1. Introduction

Visual organs are crucial for survival in animals. Due to visual tasks, including predation, avoidance of enemies, movement and reproduction, the visual organs of some animals have evolved special features such as stereoscopic vision (Nityananda et al., 2018), peripheral vision (Banks et al., 2015), rapid saccade (Jonathan et al., 2019) and visual illusion (Endler et al., 2010). Visual organs of some animals have even evolved to recognize peculiar optical signaling, such as polarized light (PL) (Gagnon et al., 2015; Templin, 2017). PL is another property of natural light (NL) that is scattered during transmission, and PL can be divided into linearly polarized light (LPL), circularly polarized light (CPL) and elliptically polarized light according to the trajectory shape of PL vector (Wang et al., 2013). PL was once overlooked because the human eye can not directly identify it. However, behavioral, morphological, and electrophysiological experiments have hypothesized that PL can help animals with polarization-sensitive visual system enhance the contrast between objects and the environmental background (Shashar et al., 2011, Marshall and Cronin, 2014), thereby "secretly" conducting directional navigation (Homberg, 2015), camouflage (Chiao et al., 2011), target detection (How et al., 2015), mate selection (Calabrese et al., 2014), and other visual tasks. It is worth noting, though, that polarization sensitivity is not the same as polarization vision. The difference lies in whether animals can accurately discern the angle of light after detecting PL (Templin, 2017). That means there are fewer animals with polarization vision, especially CPL vision (CPLV). Although the wings of golden turtle beetles seem to have the ability to reflect CPL (Brady and Cummings, 2010; Jiang et al., 2012), they can't recognize it (Miklós et al., 2012). There are more than 400 mantis shrimp species (Arthropoda: Crustacea) in the world, and to the surprise of the researchers, is the only animal found to reflect and also recognize CPL (Chiou et al., 2008; Graydon, 2009; Thoen, 2014).

A previous behavioral study has found that a large proportion (up to 85%) of the Philippine mantis shrimp (*Gonodactylaceus falcatus*) show an instinctive avoidance to caves that emit CPL (Gagnon et al., 2015). The carapace (i.e. appendage, telson) of mantis shrimp has also been found to reflect CPL and the reflex ability is gender-specific (Graydon, 2009; Gagnon et al., 2015). Interestingly, CPL reflected from mantis shrimp carapace can only be recognized by members of the same or related species, which implies that CPL is a communication signaling unique to mantis shrimps (Gagnon et al., 2015). In fact, mantis shrimps spend most of their life cycle in burrows, which become their exclusive territory to effectively hide and defend themselves against enemies (Zhao et al., 2019). Therefore, it is safe to speculate that the CPL reflected in the burrow is a guard signal for mantis shrimps outside the cave that the cave is occupied by a mantis shrimp. In conclusion, it seems that CPL signaling can help mantis shrimp expand their visual field in the dark seafloor and then accurately find suitable caves, which effectively reduces competition among the ferocious mantis shrimps.

The mid-band ommatidia of compound eye are the critical structure for the mantis shrimp to recognize

Posted on 30 Aug 2023 — The copyright holder is the author/funder. All rights reserved. No reuse without permission. — https://doi.org/10.22541/au.169339743.30080820/v1 — This a preprint and has not been peer reviewed. Data may be preliminary.

Posted on 30 Aug 2023 — The copyright holder is the author/funder. All rights reserved. No reuse without permission. — https://doi.org/10.22541/au.169339743.30080820/v1 — This a preprint and has not been peer reviewed. Data may be preliminary.

CPL (Marshall, 1988). Previous morphological studies on the mantis shrimp (i.e. *Odontodactylus cultrifer* , *Lysiosquillina maculate*) compound eyes have shown that the angle between the direction of the distal rhabdom of R8 retinular cell and the proximal rhabdom of (R1, 4, 5) and (R2, 3, 6, 7) retinular cells in the mid-band ommatidia was +45° and -45°, respectively (Marshall, 1988; Chiou et al., 2008; Graydon, 2009). Meanwhile, the distal rhabdom of R8 retinular cell shows a special short oval shape and can act as a quarter-wave plate (Chiou et al., 2008). This impressive array of rhabdom array and shape can convert CPL received by R8 retinular cell into LPL that can be easily recognized by R1˜R7 retinular cells (Graydon, 2009; Gagnon et al., 2015). Additionally, the duplication of opsin genes and parallel substitution of functional amino acid sites that are positively selected for CPL may also be responsible for the CPLV of the mantis shrimp (Yuan et al., 2010; Briscoe et al., 2010). In the mid-band retinular cells of the *Gonodactylus smithii* and *Odontodactylus scyllarus* compound eyes, there are 6 middle wavelength opsins (MWSs) and 15 *MWS* genes have been confirmed (Porter et al., 2009; Cronin et al., 2010). Meanwhile, Porter et al. (2009) speculated that the mantis shrimp has also undergone*MWS* genes duplication during the CPL adaptation, and new*MWS* genes with CPL recognition function have been generated, but these theories have not been proven.

As a representative of the mantis shrimp, *Oratosquilla oratoria*(De Haan, 1844) is widely distributed in the coastal waters of China and has highly developed compound eyes. Although the mid-band of the*O. oratoria* compound eye only has two rows of ommatidia (Marshall et al., 2007; Fu et al., 2019; Zhao et al., 2019), it is still an excellent model for CPL recognition mechanism research. In this study, we aimed to elucidate the critical CPL-recognition mechanisms of the*O. oratoria* and other mantis shrimp species at the morphological and molecular levels. The microscopic structure of the *O. oratoria* compound eye was observed for the first time, and transcriptome and proteome sequencing were performed for the *O. oratoria* compound eye exposed to five lighting conditions. Here we providing key knowledge to understand the formation and evolution of CPLV and CPLV-manipulation visual tasks in mantis shrimps.

2. Materials and methods

2.1 Ethics

O. oratoria is not an endangered or protected animal in any country, and no special ethical approval are required. All *O. oratoria* s used in subsequent experiments were placed on ice for frozen anesthesia before dissection to minimize the suffering. Meanwhile, we rigorously conducted the experiments under the guidance of the National Institutes of Health Guidelines for the Care and Use of Laboratory Animals (NIH Publication No. 8023, revised in 1978) and Institutional Animal Care and Use Committee of Yantai University.

2.2 Animals

Considering that the potentially gender-specific CPL-reflection ability of mantis shrimps, the present study only focused on male *O. oratoria* . A total of 150 male *O. oratoria* s (average weight: 26.45 ± 3.11g; average length: 125.39 ± 6.15 mm) were collected in May to June 2022 from Yantai Yangma Island, China. The collected *O. oratoria* s were transported back to the laboratory using an incubator filled with seawater. All *O. oratoria* s underwent 30 days of temporary rearing in natural seawater and then were used for morphological characterization and subsequent light exposure experiments.

2.3 Microstructure examination of *O. oratoria* compound eye

To study the microstructure of the compound eye, we dissected the bilateral compound eyes of one *O. oratoria* exposed to nature light after the habituation period and removed the cornea of the compound eyes under the stereomicroscope and immersed the compound eyes in filtered seawater. The outer shell of the compound eye was removed anatomically using corneal scissors and ophthalmic forceps along the base of the eyestalk, and the remaining compound eyes were fixed in 4% paraformaldehyde for 30 minutes at room temperature. The compound eyes were dehydrated according to the following procedures: 30% ethanol (60 minutes)-50% ethanol (60 minutes)-70% ethanol (60 minutes)-95% ethanol (60 minutes)-ethanol (30 minutes)-ethanol (30 minutes)-1:1 xylene: ethanol (5 minutes)-xylene (3 minutes)-xylene (3 minutes)-paraffin (120 minutes). The

Posted on 30 Aug 2023 — The copyright holder is the author/funder. All rights reserved. No reuse without permission. — https://doi.org/10.22541/au.169339743.30080820/v1 — This a preprint and has not been peer reviewed. Data may be preliminary.

parrafin used was a mixture of equal proportions of high- and low- melting point paraffin to then use the mixture for sample embedding. The embedded compound eyes were cut into 4-micron sections using the microtome (Leica). The excised compound eyes were expanded in 37 water and then affixed to glass slides coated with poly-L-lysine (Sigma). The compound eye slices were then incubated at 37 for 12 hours before deparaffinization and rehydration according to the following procedures: xylene (10 minutes)-1:1 xylene: ethanol (3 minutes)-95% ethanol (3 minutes)-80% ethanol (3 minutes)-70% ethanol (3 minutes)-50% ethanol (3 minutes)-30% ethanol (3 minutes)-distilled water (3 minutes). After undergoing hematoxylin-eosin staining, compound eyes were sealed and stored using a sterile aqueous solution of 50% glycerol (Sangon Biotech). Finally, the transverse and longitudinal sections were examined and then photographed under digital microscope (Leica).

Additionally, to observe the surface ultrastructure of *O. oratoria* compound eye, the *O. oratoria* compound eyes were excised under the stereomicroscope (Leica) and immersed in warm water (˜40) for 2 days to achieve softening. The dirt on the surface of the compound eyes was washed in ultrasonic cleaning instrument (Skymen) for 10 minutes. The compound eyes were dehydrated in multiple gradient concentrations of ethanol (50%, 70%, 80%, 90%, 95%, and 100%) for 10 minutes, and then dehydrated 3 times continuously with absolute ethanol. After the compound eyes were dried at room temperature, they were glued to the sample stage with the help of a stereoscopic microscope (Nikon) and conducting resin (Ausbond) by adjusting the sample orientation slightly with tweezers. The compound eyes were sprayed with gold in the sputter coater (Cressington) and photographed under the scanning electron microscopy (ZEiSS) to scan the surface ultrastructure. Meanwhile, the internal ultrastructure of the*O. oratoria* compound eye with the cornea removed was observed by referring to the surface ultrastructure observation process mentioned above.

Finally, to observe the refined structure of the rhabdom of *O. oratoria* compound eye, we immobilized the cornea-removed compound eyes with 5% glutaraldehyde for 2 hours and then applied phosphate buffer to the fixed compound eyes three times for 30 minutes each time. The treated compound eyes were re-fixed with 2% osmic anhydride for 90 minutes and rinsed with phosphate buffer. The compound eyes were then dehydrated using the subsequent processes: 30% ethanol (5 minutes)-50% ethanol (5 minutes)-70% ethanol (10 minutes)-80% ethanol (10 minutes)-85% ethanol (15 minutes)-90% ethanol (15 minutes)-95% ethanol (15 minutes)-100% ethanol (20 minutes)-100% ethanol (20 minutes)-acetone (15 minutes)-acetone (15 minutes). Subsequently, Epon 812 and epoxy-coated compound eyes were cut into ultrathin (50 nm) sections using the diamond knife and then stained with saturated uranyl acetate and citric acid (PH = 12). Finally, the sections were observed and photographed using transmission electron microscope (JEOL).

2.4 Light exposure experiments

After 30 days of temporary rearing in natural seawater, 90 healthy*O. oratoria* s were randomly transferred to 15 separated circulating tanks. 15 tanks were divided into five lighting scenarios (dark [DL], natural light [NL], linearly polarized light [LPL], left-rotation CPL [LCPL], and right-rotation CPL [RCPL]) by matching light sources and polarizers, and 3 tanks were present for each lighting scenario. We used light-tight boxes to envelop the 15 tanks to avoid external light affecting the set lighting scenarios. Meanwhile, 6 *O. oratoria* s were reared in each tank for 7 days in each scenario (Figure.1). During the experimental period, clams were fed to avoid cannibalism among the *O. oratoria* s per tank and the seawater was changed every day. Additionally, it is worth noting that because half of the *O. oratoria* s in the LPL scenario died, the culture experiment in the LPL scenario was repeated three times to ensure the number of samples required for transcriptome and proteome sequencing.

Posted on 30 Aug 2023 — The copyright holder is the author/funder. All rights reserved. No reuse without permission. — https://doi.org/10.22541/au.169339743.30080820/v1 — This a preprint and has not been peer reviewed. Data may be preliminary.

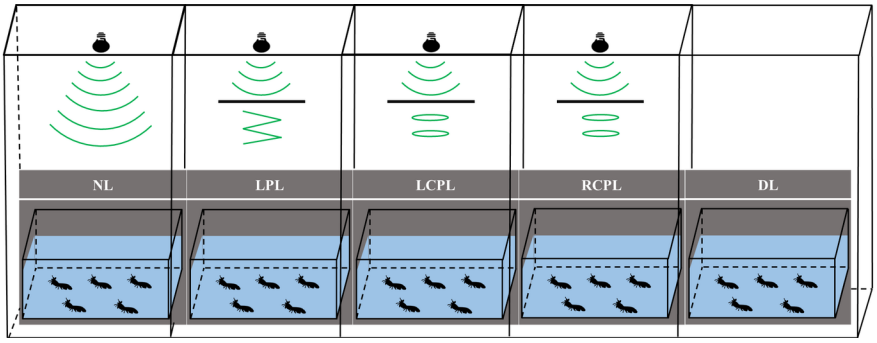

Figure.1. Experimental setup for light exposure experiment including lighting scenarios settings. The light source comes from above the tank, and different types of polarized light plates convert natural light into different polarized lights. NL: natural light, LPL: linearly polarized light, LCPL: left-rotation circularly polarized light, RCPL: right-rotation circularly polarized light, DL: dark.

2.5 Compound eyes sampling, RNA, and protein extraction

After the exposure experiment, the fresh compound eye mixture of 3 *O. oratoria* s in each tank were used for mRNA extraction, and the compound eye mixture of the remaining 3 *O. oratoria* s were used for total protein extraction. The mRNA extraction processes were as follows: Liquid nitrogen is added to the individual sample and fully ground, and the high-quality total RNA (The RNA integrity number detected by Agilent 2100 bioanalyzer is greater than 7) was extracted using the standard Trizol Reagent Kit (Sangon Biotech). Subsequently, we use RNA purification Beads (Illumina) to adsorb the mRNA from total RNA and then use Beads Binding Buffer (Illumina) to clean the adsorbed mRNA three times. The eluted mRNA was incubated at 94°C for 8 minutes to achieve mRNA purification. The total protein extraction processes were as follows: SDS lysate (Macklin) was added to the individual sample that were fully ground with liquid nitrogen to promote complete sample cleavage. PMSF (ThermoFisher) was added to the lysed sample to inhibit protein hydrolysis. The solution was ultrasonically broken 3 times on ice, and the total protein was then obtained in the supernatant by centrifugation.

2.6 Identification of circularly polarized light (CPL) recognition-related functional genes and proteins

The purified mRNA was cleaved into appropriate size fragments using the Fragmentation buffer (Agilent) and then used for cDNA libraries construction. We sequenced all cDNA libraries using the Illumina NovaSeq 6000 sequencing platform across one lane with paired-end 150 bp. The raw transcriptome sequencing reads were trimmed using fastp software (version 0.20.1; Chen et al., 2018) and low-quality paired-end sequencing reads with sequencing adaptors, unknown nucleotide (ratio $>$ 10%), and low quality (if Q_{phred} [?] 20 over 50%) were eliminated. The high-quality sequencing reads from 15 *O. oratoria* s were then*de novo* assembled to unigene sequences by Trinity (version 2.0.6; Grabherr et al., 2011) software (Supplementary Material). The BUSCO software (version 3.0.2; Simao et al., 2015) was evaluated for the completeness of the assembled unigene sequences (Supplementary Material). We set the lighting scenario as an independent variable and then used BWA-mem (Li and Durbin, 2009) to map each set of high-quality sequencing reads to the unigenes sequences to calculate the gene expression level of the *O. oratoria* compound eyes in the 5 lighting scenarios. FPKM (Fragments per kilobase of exon model per million mapped fragments) values (Langmead and Salzberg, 2012) were used to normalize the gene expression levels. Considering that the expression variation of functional genes will affect the response ability of the *O. oratoria* compound eye to different lighting scenarios, we treated the FPKM of the *O. oratoria* s compound eyes under DL as a control and then quantified the differentially expressed genes (DEGs) of the compound eyes exposed to other four lighting scenarios (NL, LPL, LCPL, and RCPL) using edgeR package (Lou et al., 2019). The filtering thresholds for significantly DEGs were conservative and as follows: false discovery rate (FDR) [?] 0.01 and $|\log_2\text{FoldChange}|$ [?] 2. To verify the

Posted on 30 Aug 2023 — The copyright holder is the author/funder. All rights reserved. No reuse without permission. — https://doi.org/10.22541/au.169339743.30080820/v1 — This a preprint and has not been peer reviewed. Data may be preliminary.

reliability of the transcriptome data, we screened 11 opsin genes (Table.1) and then performed quantitative reverse transcription PCR (qRT-PCR) experiments. Two stably expressed reference genes (*EΦ1a*and *Tubu*) were applied to correct eleven target genes. Primer Premier 6.0 software was used to design the 11 target genes- and 2 reference genes- specific primers (Table.1). The 15 mRNAs used for transcriptome sequencing were reverse-transcribed into cDNA and diluted 25 times to obtain cDNA templates for qRT-PCR experiments. All the qRT-PCR experiments were performed on the CFX96 Touch Real-Time PCR Detection system following the instructions of QuantiNova SYBR Green PCR Kit. Three technical replicates were carried out for each qRT-PCR reaction, and $u2^{-\Delta\Delta^{\sim}T}$ ($\Delta CT = CT_{\text{target genes}} - CT_{\text{reference gene}}$, $\Delta\Delta CT = \Delta CT_{(NL,\ LPL,\ RCPL,\ LCPL)} - \Delta CT_{NL}$) was used to calculate the relative expression of 11 target genes.

Table.1. Primer sequences specific to reference genes and target genes.

	Transcript_id	Gene name	Primer (5' to 3')	Product length
Reference genes	-	*EΦ1a*	For_AATCTGGTGATGCTGCTATGG	123bp
			Rev_CAACAGCCACTGTCTGTCTCAT	
	-	*Tubu*	For_AACACCGACGAGACATACTGC	150bp
			Rev_ACCTGGGAATCGGAGACAAG	
DEGs	Cluster-42753.40296	*ARR I*	For_AGAAACTGGGACCAAACG	118bp
			Rev_GAGTATTCAACACCGCAAG	
	Cluster-42753.38248	*ARR II*	For_TCGGGACTTCGTAGACAA	149bp
			Rev_GCAAGCCCATAACTTCATC	
	Cluster-42753.26866	*CYAB*	For_ACCTTCCACCGCACTTTC	124bp
			Rev_CAATCTTGATGACCCGTTCT	
	Cluster-42753.31906	*LWS I*	For_CACGACCTGGTGTTACTTCC	113bp
			Rev_CCATCTTCTTAGCCTGTTCC	
	Cluster-42753.37563	*LWS III*	For_TCTACACTGCCTGGGTCTT	164bp
			Rev_CTCGTTGGAGGTCTGCTT	
	Cluster-42753.37549	*TRPC*	For_GGCGGAGAAATCAACGAA	199bp
			Rev_ATAGAGGCGATGGCGAAG	
	Cluster-42753.45119	*MYO III*	For_CTCTTCCCTCGGTCTGGT	113bp
			Rev_GACACTGCCGCTACTTCG	
	Cluster-42753.42664	*MYO XV*	For_AGAAGAGCGACGAGTAGAGG	103bp
			Rev_ATTACCGAGGCGAGGAAC	
	Cluster-42753.35592	*UV*	For_TTTCAGTGATGGGATGCT	251bp
			Rev_TTCGTCGTCCGTAAGATAG	
	Cluster-42753.11073	*GPR*	For_CGTGGGCTCCTTGGTCAGT	119bp
			Rev_GGGCGGTTCCTTCTTGCT	
	Cluster-42753.24786	*RRH*	For_ATGGGGAGGGAATCGTC	83bp
			Rev_TCCGTGCCAACCAAGAG	

The Bradford protein quantitative kit was used to measure the concentration of each protein. Lysis buffer, trypsin and TEAB buffer were added to each protein and digested at 37 °C overnight. Equal volume of 1% formic acid was mixed with digested protein and then centrifuged. The supernatant was slowly loaded to the C18 desalting column for desalting, followed by washing, elution and lyophilized of the protein. Equal volumes of mixed peptide samples were fractionated using high pH reverse-phase high performance liquid chromatography (HPLC) coupled with an Agilent 300 Extend C_{18} column (5 μm particles, 4.6 mm ID, 250 mm length) (Wu et al., 2010). Finally, purified peptide samples with the removal of non-specific adsorbed peptides were collected and lyophilized for liquid chromatograph-mass spectrometer/mass spectrometer (LC-MS/MS) detection (Hu et al., 2018). We extracted the coding region sequences from the transcript assembled above using TransDecoder (Lou et al., 2018) and then constructed the specified database to search the MS/MS profiles from each run, and further quantified for peptide spectrum matches (PSMs) and proteins

Posted on 30 Aug 2023 — The copyright holder is the author/funder. All rights reserved. No reuse without permission. — https://doi.org/10.22541/au.169339743.30080820/v1 — This a preprint and has not been peer reviewed. Data may be preliminary.

using Proteome Discoverer 2.4 software with SEQUEST® search engine. In order to reduce the false positive rate, the above-mentioned search results were further filtered by Proteome Discoverer 2.4 software, and those PSMs with confidence greater than 99% were considered as credible PSMs, and those proteins containing at least one unique peptide were considered as credible proteins. A further significance cutoff of FDR < 0.1 was used for PSMs and proteins. We analyzed the relative quantitative value of each PSM in 15 samples according to the MS peak area, and then obtained the relative quantitative value of the unique peptide according to the PSM relative quantitative value of each peptide (Supplementary Material). Furthermore, the relative quantitative value of each protein was identified based on the quantitative information of unique peptides contained in each protein (Plubell et al., 2017). To explore the proteins involved in CPL recognition, we used the relative quantitative value of proteins in the *O. oratoria* compound eyes exposed to the DL as a control and determined the differentially expressed proteins (DEPs) in comparison to the samples exposed to the other four lighting scenarios (NL, LPL, LCPL, and RCPL). T-test was used to identify significantly DEPs with a p-value of less than 0.05 (Liu et al., 2020). To verify the reliability of the proteome data, we selected known opsin proteins important in light recognition and carried out the subsequent quantitative analyses. Firstly, peptides were collected using data-dependent acquisition (DDA) mode to generate mass spectrometry raw data, and Proteome Discoverer software (version 2.2) was used to search the generated mass spectrometry data to obtain the unique peptides of each target protein. Parallel reaction monitoring (PRM) was used to scan the candidate peptides. Meanwhile, an equal amount of reference peptide (DSPSAPVNVTVR, the red "V" is the heavy isotope marker) was added to each sample to correct the peak area. The chromatographic peak of target peptide was extracted by Skyline software and three daughterions with high peptide abundance were selected for quantitative analyses. Finally, the peak areas of target peptides were adjusted according to the peak area of reference peptide to obtained the relative expression of each peptide in each sample.

Furthermore, integrate transcriptome and proteome information to identified the DEGs and DEPs with high correlation in each comparison paired according to Person correlation coefficient.

Finally, we performed gene function and metabolic pathway enrichment analyses for significant DEGs and DEPs based on Gene Ontology (GO; Di Lena et al., 2015) and Kyoto Encyclopedia of Genes and Genomes (KEGG; Kanehisa et al., 2004) databases to determine which biological functions are involved in CPL perception. All annotation results were visualized using R (version 4.2.2).

3. Results

3.1 Compound eye morphology

The *O. oratoria* has a pair of oval compound eyes that are symmetrically distributed on both sides of the head. The compound eye is composed of multiple orthohexagnal ommatidia with similar area and the width of each ommatidium is about 800 μm (Figure.2-H). Two rows of mid-band ommatidia are present in the compound eye (Figure.2-G). Each ommatidium is composed of cone cells that converge photon, pigment cells that recognize color, and retinular cells that convert light signals from the outside to the inside (Figure.2-A-J). Meanwhile, the retinular cells were structurally like that of other crustaceans and contained 2 cell types. The surface of retinal cells is lined with numerous horizontal microvilli, which are aggregated to form rhabdom arrays (Figure.2-A-L). We captured the square and oval of rhabdom (Figure.2-E, K, and J), and we speculate that they may be proximal and distal rhabdom, respectively. Additionally, we also found that the microvilli from different retinular cells are arranged in a cross-over pattern (Figure.2-K, and J).

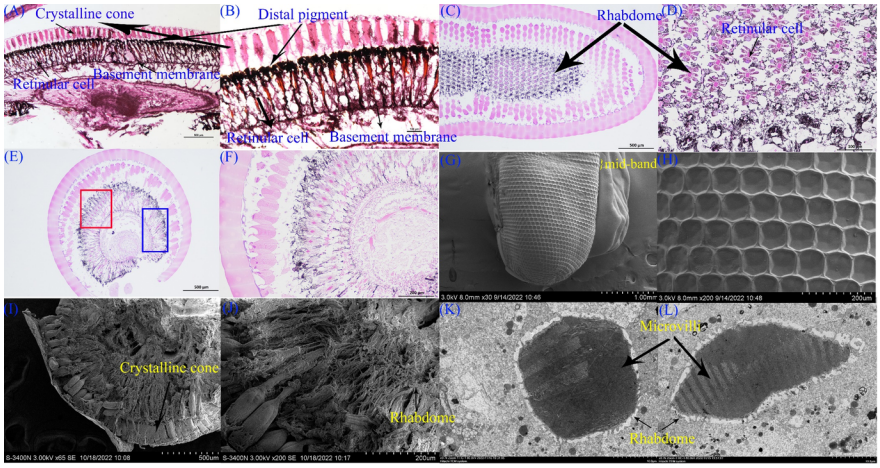

Figure.2. External and internal morphology of the *O. oratoria*compound eye. Note: (A) – (F) represents paraffin sections of different profiles. (G) and (H) represents the surface ultrastructure. (I) and (J) represents the internal ultrastructure. (K) and (L) represents the refined rhabdom structure.

3.2 Potential CPL recognition regulation mechanism

We hypothesized that the expressions of vision-related genes and proteins in the DL would not be effective and could serve as a control value, results showed that NL revealed the largest number of DEGs (1259) and DEPs (90) when compared to DL. This was followed by LCPL with 334 DEGs and 76 DEP and RCPL with 259 DEGs and 67 DEPs. The lowest number of DEGs (85) and DEPs (50) was found for LPL (Figure.3).

Posted on 30 Aug 2023 — The copyright holder is the author/funder. All rights reserved. No reuse without permission. — https://doi.org/10.22541/au.169339743.30080820/v1 — This a preprint and has not been peer reviewed. Data may be preliminary.

Posted on 30 Aug 2023 — The copyright holder is the author/funder. All rights reserved. No reuse without permission. — https://doi.org/10.22541/au.169339743.30080820/v1 — This a preprint and has not been peer reviewed. Data may be preliminary.

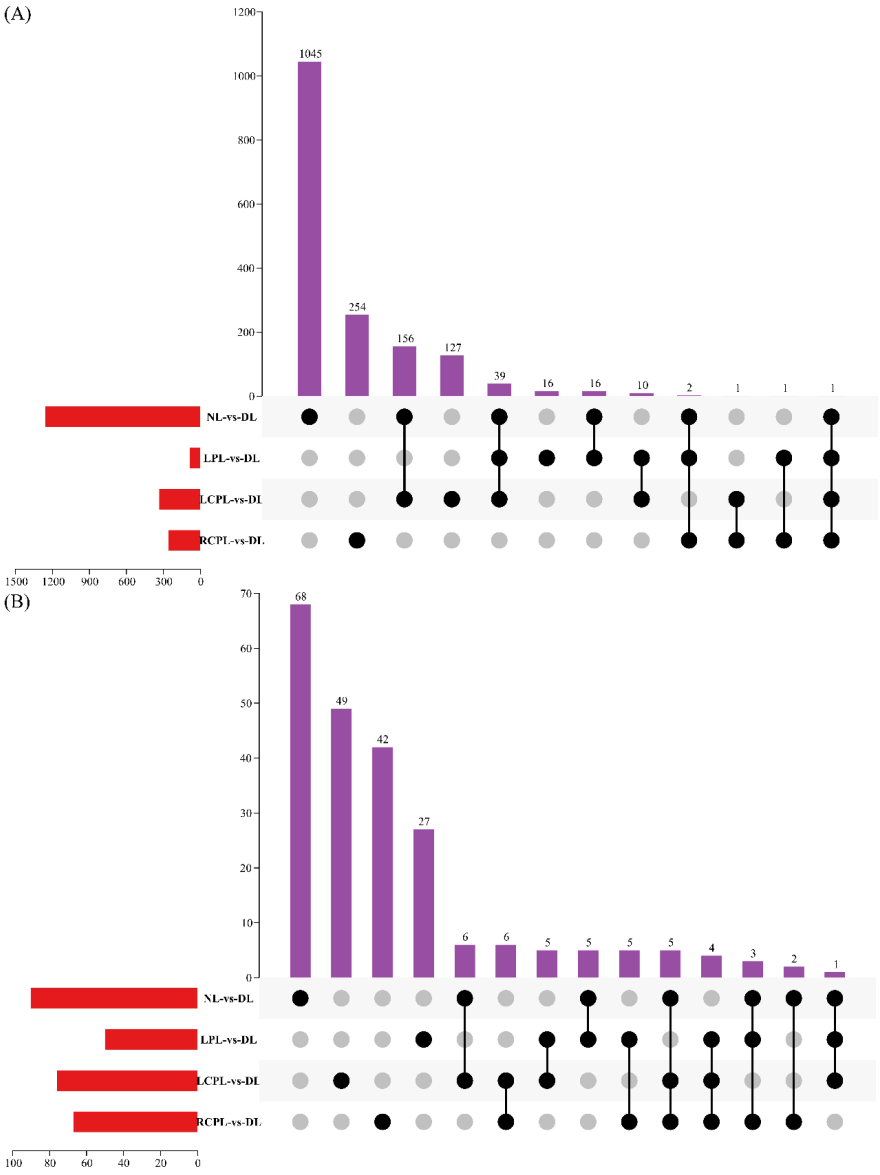

Figure.3. The number of differentially expressed genes (A) and proteins (B) among four experimental pairs. Note: The red bars represent the number of DEGs and DEPs among four experimental pairs. The purple bar represents the number of shared or specific DEGs and DEPs of the four experimental groups.

The opsin - (*LWS I* , *LWS II* , *SWS I* , *SWS II* ,*ARR I* , *ARR II* , *TRPC* , *HISC* , *SLC* ,*KCNKN* , *RRH* , and *CYAB*) and microvilli - related DEGs (*MYO III* and *MYO XV*) were mostly differentially expressed when exposed to NL and LCPL, while LPL scenario showed the lowest gene expression (Figure.4). Although 259 DEGs were found in the RCPL (Figure.3), they did not annotate to vision-related functional genes. It is worth noting that we found significant differences in the expression levels of *LWS I* , *LWS III* , *SWS I* , *SWS II* , *MYO III* , *ARR I* ,*ARR II* , and *TRPC* in the comparison between LCPL and DL (Figure.4).

Posted on 30 Aug 2023 — The copyright holder is the author/funder. All rights reserved. No reuse without permission. — https://doi.org/10.22541/au.169339743.30080820/v1 — This a preprint and has not been peer reviewed. Data may be preliminary.

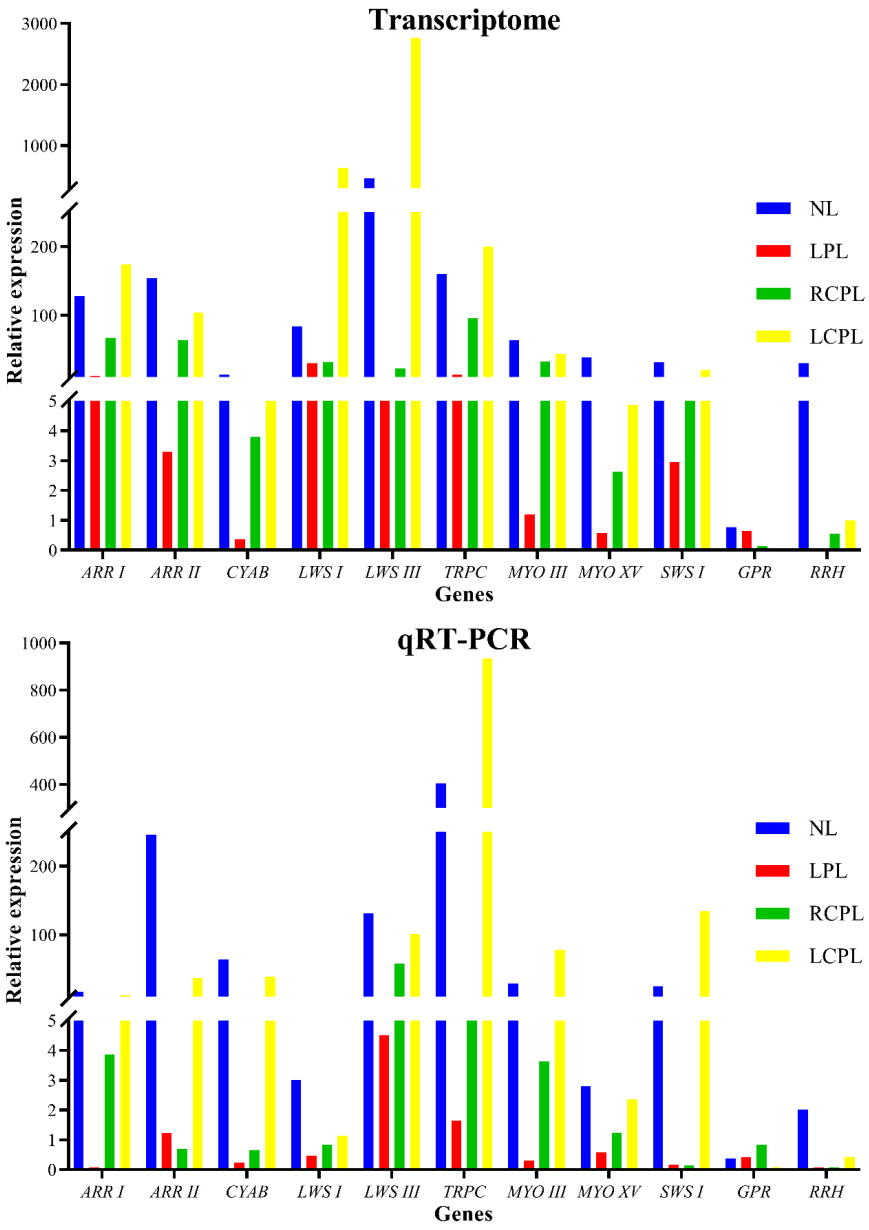

Figure.4. The expression trend of 11 vision-related functional genes of *O. oratoria* compound eyes in five lighting scenarios based on transcriptome and qRT-PCR datasets.

Meanwhile, few vision-related functional proteins were identified, including arrestin protein, sodium-coupled neutral amino acid transporter protein, sodium/potassium/calcium exchanger protein, transient receptor potential channel protein, retinal dehydrogenase protein, and G protein-coupled receptor protein. Among them, arrestin protein and sodium-coupled neutral amino acid transporter protein were inferred to contribute to the LCPL-recognition of *O. oratoria* compound eye. The expression trends of five proteins based on proteomic sequencing and PRM were consistent. Similar to gene expression levels, the expression levels of vision-related proteins in *O. oratoria* compound eyes exposed to NL or LCPL scenarios showed the higher values (Figure.5).

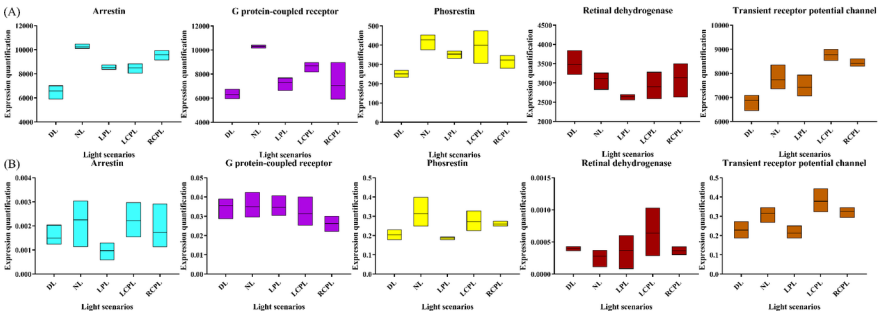

Figure.5. The expression quantification of 5 vision related functional proteins of *O. oratoria* compound eyes in five lighting scenarios based on a) proteome and b) PRM datasets. The upper, lower, and middle lines of each box represent the maximum, minimum, and median values, respectively.

3.3 Correlation analyses of the proteome and transcriptome

Association analyses of the transcriptome and proteome data were performed to explored the recognition nature of *O. oratoria*compound eyes to CPL. A total of 11, 8, 8, and 12 DEGs and DEPs with high correlation existed in NL-vs-DL, LPL-vs-DL, LCPL-vs-DL, and RCPL-vs-DL, respectively. According to the annotation information, only 1 LCPL recognition-related DEG and DEP were identified as highly correlated and they are annotated as *TRPC* gene and transient receptor potential channel protein, respectively. Meanwhile, *TRPC*gene and transient receptor potential channel protein are implicated in the biological function of ion transmembrane transporter activity, and their products are involved in phototransduction pathway (Figure.6).

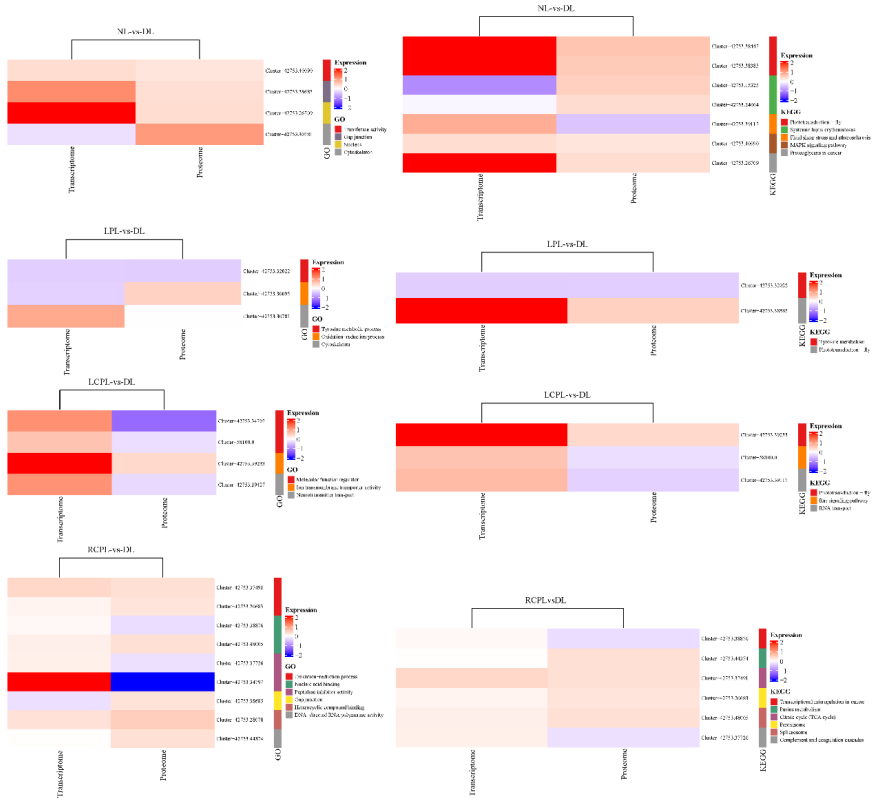

Posted on 30 Aug 2023 — The copyright holder is the author/funder. All rights reserved. No reuse without permission. — https://doi.org/10.22541/au.169339743.30080820/v1 — This a preprint and has not been peer reviewed. Data may be preliminary.

Figure.6. The GO and KEGG annotation information of DEGs and DEPs with high correlation. Note: The left to right elements of each heatmap represent functional genes, functional proteins, unigene sequence IDs, GO/KEGG enrichment results, expression level of functional genes/proteins (upside), and full-name of GO terms/KEGG pathways (downside).

4. Discussion

Recognition of CPL is a unique and fascinating phenomenon in the animal kingdom. In this study we reveal the micro-regulatory mechanisms of how a mantic shrimp such as *O. oratoria* can recognize CPL.

4.1 The refined structure of the compound eye is responsible for the CPLV

In order to improve the capture and absorption efficiency of CPL, the mantis shrimp compound eye has inevitably evolved the morphological features that can enhance CPL sensitivity (Honkanen et al., 2014). The *O. oratoria* compound eye is divided into two almost perfectly symmetric halves by a mid-band to create triphasic vision, but the mid-band with CPL-recognition consists of only two rows of ommatidia, which is sparse compared to the many mantis shrimps (such as Gonodactyloidae) (Marshall, 1988; Chiou et al., 2008; Graydon, 2009; Templin, 2017). Thus, we speculate that the CPLV of *O. oratoria* may be weakened. Previous study confirmed that the PL in water is predominately caused by the scattering of various particles (Ivanoff and Waterman, 1958, Cronin et al., 2003), and the polarization degree of light in turbidity water (usually not above 30%) was significantly lower than that in clear water (reach to 60%) (Ivanoff and Waterman, 1958, Cronin et al., 2003). *O. oratoria* are known to live in relatively high turbidity environments and thus may experience less CPL throughout its evolutionary process than other mantis shrimp species living in relatively clear water, which indirectly leads to the "disuse" of CPLV-related mid-band in *O. oratoria* .

The relatively large ommatidium area (width ˜ 800 μm) appears to enhance the capture efficiency of *O. oratoria* compound eye to photon (McIntyre and Caveney, 1998). Although we did not perform the validation experiment for ommatidia function in *O. oratoria* , related study has been accurately established in the ommatidia of other mantis shrimps (Templin, 2017). Each ommatidium resembles a cylindrical structure, which also increases the possibility of photon capture. We observed that the microvilli in the rhabdom are orthogonal geometric interleaved, this array has been proved to be very valuable for the transmission and recognition process of CPL due to it can facilitates the ability to detect two or more e-vector orientations (Kleinlogel, 2006; Templin, 2017). It is worth noting that two different shapes (square and oval) of rhabdom were captured in the electron microscopic section of ommatidia, which may be derived from R1-7 and R8 retinular cells, respectively (Liu and Ding, 2015). Previous studies have demonstrated that the short oval rhabdom can act as a quarter-wave plate and convert the received CPL into LPL (Cronin et al., 1991). Hence, the *O. oratoria* compound eye has microstructures that can recognize CPL, and these structures can ensure that the compound eye can accurately distinguish the angle of light after detecting CPL, and convert CPL into easily recognized LPL.

4.2 The potential order of light utilization by *O. oratoria* compound eye

The expression levels of vision-related functional genes and proteins are light scenario-specific, so the identified DEGs and DEPs may regulate the light recognition process of *O. oratoria* compound eye. Based on the annotation information, visual regulation-related DEGs and DEPs mainly appear in NL-vs-DL and LCPL-vs-DL, especially in NL-vs-DL. This may mean that *O. oratoria* compound eye use NL and LCPL over LPL and RCPL, although LCPL needs to be converted to LPL for further recognition. This is puzzling because any areas (whether dorsal, ventral, or midband) of the mantis shrimp compound eye have been shown to recognize the LPL (Marshall, 1988; Chiou et al., 2008; Graydon, 2009; Templin, 2017). Meanwhile, orthogonal geometric interlace rhabdom were also found in the *O. oratoria* ommatidia, suggesting that the *O. oratoria* has the LPL recognition ability. There may be two explanations for this, including (1) the lack of reference genome for *O. oratoria* or other mantis which limited the comparative transcriptomic and proteomic analyses, and no annotations were found for functional genes or proteins that can recognize LPL. (2) LPL is an "ecological trap (Dwernychuk and Boag, 1972)" of *O. oratoria* , which is a very bold hypothesis without further proof. In fact, we repeated three breeding experiments and found that the mortality rate

Posted on 30 Aug 2023 — The copyright holder is the author/funder. All rights reserved. No reuse without permission. — https://doi.org/10.22541/au.169339743.30080820/v1 — This a preprint and has not been peer reviewed. Data may be preliminary.

Posted on 30 Aug 2023 — The copyright holder is the author/funder. All rights reserved. No reuse without permission. — https://doi.org/10.22541/au.169339743.30080820/v1 — This a preprint and has not been peer reviewed. Data may be preliminary.

of*O. oratoria* s exposed to LPL was close to 50%, while the mortality rate of *O. oratoria* s exposed to other light scenarios was almost 0. Therefore, we suspected that the "ecological trap" caused by LPL is more likely to be a behavioral phenomenon of*O. oratoria* (Battin, 2004; Robertson and Hutto, 2006). Specifically, the attractiveness of LPL to*O. oratoria* may not be commensurate with its suitability for survival and reproduction (Levins, 1968, Witherington, 1997), and may even lead to the death of mantis shrimp. This "polarization captivity effect" has been demonstrated in a variety of animals and are responsible for their continued death (Kriska et al., 2006; Horváth et al., 2011; Robertson et al., 2017), but was not measured here. While further research and validation is needed, from our results we speculate that the order of light utilization by *O. oratoria* compound eye is NL, LCPL, LPL, RCPL and DL.

4.3Opsin is the first stage of CPL perception

We found significant changes in the expression of some opsin genes and related proteins in *O. oratoria* compound eyes exposed to LCPL, suggesting that opsin is critical for CPL recognition in *O. oratoria* compound eye. Photon acquisition and absorption by opsin initiates the visual transduction cascade mechanism (Zang and Neuhauss, 2021), the physical stimuli generated by photons are subsequent converted into biological signals and then regulate the neurotransmitter glutamate released by photoreceptor synapses (Burns and Maylor, 2001; Lamb and Pugh, 2006; Fu and Yau, 2007), which will ultimately be received by the brain. In this process, opsins belonging to the G protein–coupled 7-transmembrane receptor family are typically covalently bound to retinal-binding proteins (formed by vitamin A1 11-cis-retinal and Schiff base) to form photopigment complexes called visual pigment (Figure.7; Farrens et al., 1996; Bowmaker and Hunt, 2006; Liu et al., 2007; Peña et al., 2016).

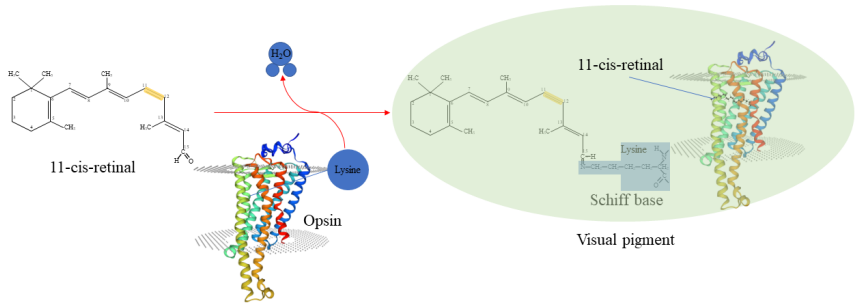

Figure.7. Schematic diagram of rhodopsin transformation.

In the present study, long-wavelength sensitive *LWS I* and*LWS II* were found to be up-regulated in the *O. oratoria*compound eye exposed to LCPL and we speculate that this is related to the shallow-water life habit of*O. oratoria* (Sealifebase database). It is well-known that the penetration of long-wavelength light is not strong and thus it is mainly concentrated in the upper water (Chen et al., 2014). Both ultraviolet (UV)-sensitive *SWS I* and blue-sensitive*SWS II* were also up-regulated in the *O. oratoria* compound eye exposed to LCPL. The polarization pattern in the UV and blue-ray have been speculated to be more stable and still trustworthy even in caliginous environment (Barta and Horváth, 2004; Horváth and Varjú, 2004). Meanwhile, both R7 and R8 retinular cells are UV-sensitive (Labhart and Meyer, 1999), and this property has been demonstrated to contribute to polarization vision in *Musca domestica* (von Philipsborn and Labhart, 1990) and *Schistocerca gregaria* (Schmeling et al., 2014). Accordingly, the *SWS I* and*SWS II* of the *O. oratoria* compound eye may be commonly used to detect the shorter-wavelength LCPL, and similar result

Posted on 30 Aug 2023 — The copyright holder is the author/funder. All rights reserved. No reuse without permission. — https://doi.org/10.22541/au.169339743.30080820/v1 — This a preprint and has not been peer reviewed. Data may be preliminary.

has been confirmed in *Neogonodactylus oerstedii* (Portera et al., 2020). We also found *ARR I* , *ARR II* , *TRPC* , *HISC* and*SLC* to be up-regulated in the *O. oratoria* compound eye exposed to LCPL. The arrestin proteins encoded by the *ARR I* and *ARR II* have long been shown to control visual transduction cascades by deactivating the phosphorylated photopigments (Wilden et al., 1986; Liu et al., 2017), and thus the increased arrestins could maintain the animal's ability to respond to light continuously (Renninger et al., 2011; Zang and Neuhauss, 2021). The transient receptor potential (TRP) channel involved by *TRPC* gene and histamine-gated chloride (HCL) channel involved by *HISC* gene are Ca^{2+} and Cl^- permeable channels with pore canal, respectively, and have been shown to regulate the opening of cyclic nucleotide-gated ion channels during optical signaling and ultimately affect the photosensitivity (Geng et al., 2002; Leung et al., 2007). In fact, up-regulation of ion channel-related genes can result in a positive influence on retinal current, suggesting that ion channel-related genes are critical for the LCPL visual transmission (French et al., 2015). Notably, we identified another gene (*KCNKN*) involved in ion channel regulation in the *O. oratoria* compound eye exposed to NL scenario. The *KCNKN* gene with K^+ exchange function can balance the efflux/influx of Ca^{2+} in response to light stimulation, thus maintaining moderately high intracellular Ca^{2+} concentration (Sakurai et al., 2016; Vinberg et al., 2017). Additionally, the expression of *RRH*and *CYAB* were only up-regulated in the *O. oratoria*compound eye under NL scenario. *RRH* -encoded peropsin is a chromophore like 11-cis-retinal, which can be bound to the all-trans retina and generate the 11-cis retina form under light stimulation (Koyanagi et al., 2002; Nagata et al., 2010). Therefore, peropsin can activate the transducin and has the function of light-sensing G protein-coupled receptors (Nagata et al., 2018).*CYAB* gene encodes the α-crytallin that has been shown to maintain crystalline lens transparency and phototaxis in vertebrates (Posner et al., 2012). Meanwhile, *CYAB* gene and *sHSP* (small heat shock protein) gene have also been confirmed to be sequentially homologous and possess molecular chaperone activity, which can be used to maintain the solubility of opsin and eventually effectively reduce light scattering in the *O. oratoria* compound eye.

Based on the potential function molecular responses of DEGs and DEPs described above, we can infer the CPLV transduction cascade processes in *O. oratoria* compound eyes (Figure.8). After the *O. oratoria* compound eye senses the LCPL, the 11-cis-retinal of the visual pigment isomerizes to trans-retinal and then detaches from shortwave opsin to activate shortwave opsin. Activated-shortwave-opsin is phosphorylated by G protein-coupled receptor kinase (GPK) and then binds to the transducin (T) that binding guanosine diphosphate (GDP). Subsequently, guanosine triphosphate (GTP) is exchanged with the GDP of the above complex and further produces T-GTP for activating the cyclic guanosine monophosphate-specific phosphodiesterase (cGMP-PDE). The protons produced by the hydrolysis of activated cGMP-PDE can inhibit sodium ion channels, resulting in nerve impulses and ultimately forming CPLV.

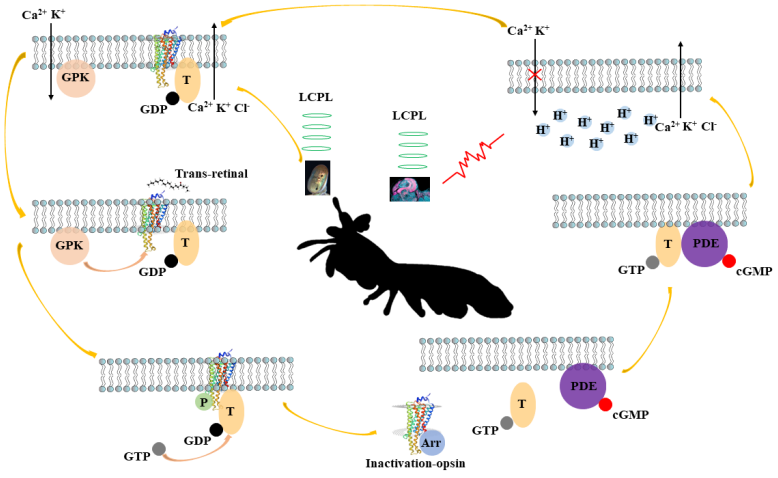

Posted on 30 Aug 2023 — The copyright holder is the author/funder. All rights reserved. No reuse without permission. — https://doi.org/10.22541/au.169339743.30080820/v1 — This a preprint and has not been peer reviewed. Data may be preliminary.

Figure.8. The inferred CPLV transduction cascade process of *O. oratoria* compound eye. Note: LCPL: left-rotation circularly polarized light. GDP: guanosine diphosphate. GPK: G protein-coupled receptor kinase. T: transducing. P: phosphorylation. GTP: guanosine triphosphate. cGMP: cyclic guanosine monophosphate. PDE: phosphodiesterase. cGMP-PDE: cyclic guanosine monophosphate-specific phosphodiesterase. Arr: arrestin protein. H^+: hydrogen ion. Ca^{2+}: calcium ion. K^+: potassium ion. Cl^-: chloride ion. The yellow arrow represents the inferred CPLV transduction cascade process. The black arrow represents the efflux/influx of ion.

4.4 CPLV depends on the shape of microvilli at the retinular cells

The microvilli are the material basis for ensuring the highly sensitive and sharp frequency-selective response to mechanoelectrical transduction (MET) generated by various stimuli (Lelli et al., 2016). A previous study confirmed that light stimulation can cause a series of changes in the ultrastructure of the compound eye, including the decrease of the diameter of the rhabdom, the disordered arrangement of microvilli, the thickening of the cytoplasm around the rhabdom, and the appearance of many organelles (i.e. multivesicular bodies, vesicular lamellar bodies, lamellar bodies and lysosomes) (Luo et al., 2006). In the present study, two genes (*MYO III* and *MYO XV*) related to the regulation of microvilli structure were found to be involved in the light adaptation of *O. oratoria* compound eye. In fact, myosins encoded by the *MYO* genes are important molecular motors that can convert the energy generated by ATP hydrolysis into kinetic energy, and have been revealed to contribute to various cellular activities of hearing and vision (Cao et al., 2011; Lelli et al., 2016). Myosins (myosin-3 and myosin-15) encoded by *MYO III* and *MYO XV* belong to the unconventional myosins, which are mainly involved in cell movement and intracellular transport of various substances (Cao et al., 2011). Circumstantially, myosin-3 protein was first discovered in*Drosophila* compound eye photoreceptor cells, and its N-terminal kinase domain can activate multiple types of light signaling elements to initiate downstream cascades that help organisms recognize light (Shieh and Zhu, 1996; Salles et al., 2009). Myosin-15 at the tip of microvilli has also been shown to be involved in the regulation of microvilli growth, and the destruction of myosin-15 often results in abnormal shortening and non-hierarchical distribution of microvilli (Delprat et al., 2005; Manor et al., 2011). Therefore, the up-regulation of*MYO* genes and myosin proteins ensures the structural integrity and correct arrangement of microvilli at the retinal cells, and promotes the conversion of LCPL optical signals into effective electrical signals in the *O. oratoria* compound eye. Another interesting discovering about the *MYO* genes is that *MYO* genes are involved in an ingenious automatic-gain control in the compound eye, in which the*MYO* genes activated by bright light can pulls pigment particles to the rhabdoms to help compound eyes adapt to bright light (Lin-Jones et al., 2009; Peña et al., 2016). Meanwhile, light-induced Ca^{2+} influx is highly effective in stimulating the motor activation of *MYO* (Satoh et al., 2008; Shen et al., 2016). It is well known that many lower animals that lack pupillary reflexes have developed pigment granules movements in response to changes in light conditions (Zang and Neuhauss, 2021). Specifically, pigment granules in the *O. oratoria*compound eye in the darkness were concentrated at the basal part of pigment cells. With LCPL exposure, the pigment granules in the *O. oratoria* compound eye will migrate to the fully light adapted position, forming a protective mechanism like “sunglasses” (Ali, 1971). Not surprisingly, *MYO III* and *MYO XV* were significantly upregulated in LCPL scenario, which may regulate the structural integrity and arrangement of microvilli in retinular cells, thereby helping *O. oratoria* compound eye to recognize LCPL.

Data and Resource Availability

All clean tanscriptome reads are available at NCBI SRA under the accession number of SRR25485440 to SRR25485454 under BioProject PRJNA1001057, and the reviewer can consult these reads through https://www.ncbi.nlm.nih.gov/sra/?term=PRJNA1001057. The mass spectrometry proteomics data have been deposited to the ProteomeXchange Consortium via the PRIDE partner repository with the dataset identifier PXD044280, and the reviewer can consult the data through follow-up information: username: reviewer_pxd044280@ebi.ac.uk; password: Y8vXxkPA.

Acknowledgements

Posted on 30 Aug 2023 — The copyright holder is the author/funder. All rights reserved. No reuse without permission. — https://doi.org/10.22541/au.169339743.30080820/v1 — This a preprint and has not been peer reviewed. Data may be preliminary.

This work was supported by the National Natural Science Foundation of China (42106128), Natural Science Foundation of Shandong Province (ZR2021QD110), and Natural Science Foundation of Zhejiang Province (LR21D060003).

Supplementary Material

Detailed information of transcriptome and proteome sequencing data.

Reference

Ali MA. 1971. Retinomotor response: characteristics and mechanisms. *Vision Res.* 11: 1225–1288. DOI: 10.1016/0042-6989(71)90010-1.

Burns ME, Baylor DA. 2001. Activation, deactivation, and adaptation in vertebrate photoreceptor cells. *Annu Rev Neurosci.* 24: 779–805. DOI: 10.1146/annurev.neuro.24.1.779.

Battin J. 2004. When good animals love bad habitats: ecological traps and the conservation of animal populations. *Conserv Biol.* 18: 1482–1491. DOI: 10.1111/j.1523-1739.2004.00417.x.

Barta A, Horváth G. 2004. Why is it advantageous for animals to detect celestial polarization in the ultraviolet? Skylight polarization under clouds and canopies is strongest in the UV. *J Theor Biol.* 226: 429–437. DOI: 10.1016/j.jtbi.2003.09.017.

Bowmaker JK, Hunt DM. 2006. Evolution of vertebrate visual pigments. *Curr Biol.* 16: 484. DOI: 10.1016/j.cub.2006.06.016.

Brady P, Cummings M. 2010. Differential response to circularly polarized light by the jewel scarab beetle *Chrysina gloriosa* . *Am Nat.* 175: 614–620. DOI: 10.1086/651593.

Briscoe AD, Bybee SM, Bernard GD, Yuan F, Sison-Mangus MP, Reed RD, Warren AD, Llorente-Bousquets J, Chiao CC. 2010. Positive selection of a duplicated UV-sensitive visual pigment coincides with wing pigment evolution in *Heliconius butterflies* . *P Natl Acad Sci USA*107: 3628–3633. DOI: 10.1073/pnas.0910085107.

Banks MS, Sprague WW, Schmoll J, Parnell JAQ, Love GD. 2015. Why do animal eyes have pupils of different shapes? *Sci Adv.* 1: e1500391. DOI: 10.1126/sciadv.1500391.

Cronin TW, Marshall NJ, Land MF. 1991. Optokinesis in gonodactyloid mantis shrimps Crustacea;Stomatopoda;Gonodactylidae. *J Comp Physiol A.* 168: 233–240. DOI: 10.1007/BF00218415.

Cronin TW, Shashar N, Caldwell RL, Marshall J, Cheroske AG, Chiou TH. 2003. Polarization vision and its role in biological signaling.*Integr Comp Biol.* 43: 549–558. DOI: 10.1093/icb/43.4.549.

Chiou TH, Kleinlogel S, Cronin T, Caldwell R, Loeffler B, Siddiqi A, Goldizen A, Marshall J. 2008. Circular polarization vision in a stomatopod crustacean. *Curr Biol.* 18: 429–434. DOI: 10.1016/j.cub.2008.02.066.

Cronin TW, Porter ML, Bok MJ, Wolf JB, Robinson PR. 2010. The molecular genetics and evolution of colour and polarization vision in stomatopod crustaceans. *Ophthal Physl Opt.* 30: 460–469. DOI: 10.1111/j.1475-1313.2010.00762.x.

Cao Y, Shen M, Zhang J, Li XD. 2011. Structure and function of Drosophila unconventional myosin. *Chinese Journal of Applied Entomology* 48: 239–246. DOI: 10.1017/S0022112010006427. (In Chinese)

Chiao CC, Wickiser JK, Allen JJ, Genter B, Hanlon RT. 2011. Hyperspectral imaging of cuttlefish camouflage indicates good color match in the eyes of fish predators. *P Natl Acad Sci USA* 108: 9148–9153. DOI: 10.1073/pnas.1019090108.

Calabrese GM, Brady PC, Gruev V, Cummings ME. 2014. Polarization signaling in swordtails alters female mate preference. *P Natl Acad Sci USA* 111: 13397–13402. DOI: 10.1073/pnas.1321368111.

Chen SL, Zhang GJ, Shao CW, Huang QF, Liu G, Zhang P, Song WT, An N, Chalopin D, Volff JN, Hong YH, Li QY, Sha ZX, Zhou HL, Xie MS, Yu QL, Liu Y, Xiang H, Wang N, Wu K, Yang CG, Zhou Q, Liao

Posted on 30 Aug 2023 — The copyright holder is the author/funder. All rights reserved. No reuse without permission. — https://doi.org/10.22541/au.169339743.30080820/v1 — This a preprint and has not been peer reviewed. Data may be preliminary.

XL, Yang LF, Hu QM, Zhang JL, Meng L, Jin LJ, Tian YS, Lian JM, Yang JF, Miao GD, Liu SS, Liang Z, Yan F, Li YZ, Sun B, Zhang H, Zhang J, Zhu Y, Du M, Zhao YW, Schartl M, Tang QS, Wang J. 2014. Whole-genome sequence of a flatfish provides insights into ZW sex chromosome evolution and adaptation to a benthic lifestyle. *Nat. Genet.* 46: 253–260. DOI: 10.1038/ng.2890.

Chen SF, Zhou YQ, Chen YR, Gu J. 2018. fastp: an ultra-fast all-in-one FASTQ preprocessor. *Bioinformatics* 34: 884–890. DOI: 10.1093/bioinformatics/bty560.

Dwernychuk LW, Boag DA. 1972. Ducks nesting in association with gulls—an ecological trap? Can. J. Zool., 50: 559–563.

Delprat B, Michel V, Goodyear R, Yamasaki Y, Michalski N, El-Amraoui A, Perfettini I, Legrain P, Richardson G, Hardelin JP, Petit C. 2005. Myosin XVa and whirlin, two deafness gene products required for hair bundle growth, are located at the stereocilia tips and interact directly. *Hum. Mol. Genet.* 14: 401–410. DOI: 10.1093/hmg/ddi036.

Di Lena P, Domeniconi G, Margara L, Moro G. 2015. GOTA: GO term annotation of biomedical literature. *BMC Bioinformatics* 16: 346. DOI: 10.1186/s12859-015-0777-8.

Endler JA, Endler LC, Doerr NR. 2010. Great bowerbirds create theaters with forced perspective when seen by their audience. *Curr Biol.*20: 1679–1684. DOI: 10.1016/j.cub.2010.08.033.

Farrens DL, Altenbach C, Yang K, Hubbell WL, Khorana HG. 1996. Requirement of rigid-body motion of transmembrane helices for light activation of rhodopsin. *Science* 274: 768–770. DOI: 10.1126/science.274.5288.768.

Fu Y, Yau KW. 2007 Phototransduction in mouse rods and cones.*Pflug Arch Eur J Phy.* 454:805–819. DOI: 10.1007/s00424-006-0194-y.

French AS, Meisner S, Liu HX, Weckstrom M, Torkkeli PH. 2015. Ttanscriptome analysis and RNA interference of cockroach phototransduction indicate three opsins and suggest a major role for TRPL channels. *Front Physiol.* 6: 207. DOI: 10.3389/fphys.2015.00207.

Fu YG, Zhu QF, Zhang YH, Yang BW, Liu ZY, Hu Y. 2019. Research on the polarization structures inspired by mantis shrimp eyes. *Infrared and Laser Engineering* 48: 9–12. DOI: 10.3788/IRLA201948.0827001.

Geng CX, Leung HT, Skingsley DR, Iovchev MI, Yin Z, Semenov EP, Burg MG, Hardie RC, Pak WL. 2002. The target of Drosophila photoreceptor synaptic transmission is a histamine-gated chloride channel encoded by ort hclA.*J Biol Chem.* 277: 42113–42120. DOI: 10.1074/jbc.M207133200.

Graydon O. 2009. An eye for inspiration. *Nat Photonics* , 3: 668.

Grabherr MG, Haas BJ, Yassour M, Levin JZ, Thompson DA, Amit I, Adiconis X, Fan L, Raychowdhury R, Zeng Q, Chen Z, Mauceli E, Hacohen N, Gnirke A, Rhind N, Palma F, Birren BW, Nusbaum C, Lindblad-Toh K, Friedman N, Regev A. 2011. Full-length transcriptome assembly from RNA-Seq data without a reference genome. *Nat Biotechnol.* 29, 644–652. DOI: 10.1038/nbt.1883.

Gagnon YL, Templin RM, How MJ, Marshall NJ. 2015. Circularly polarized light as a communication signal in mantis shrimps. *Curr Biol.* 25: 3074–3078. DOI: 10.1016/j.cub.2015.10.047.

Horvath G, Varju D. 2004. Polarized light in animal vision: polarization patterns in nature. Heidelberg: Springer.

Horvath G, Mora A, Bernath B, Kriska G. 2011. Polarotaxis in non-biting midges: female chironomids are attracted to horizontally polarized light. *Physiol Behav.* 104: 1010–1015. DOI: 10.1016/j.physbeh.2011.06.022

Honkanen A, Takalo J, Heimonen K, Vahasoyrinki M, Weckstrom M. 2014. Cockroach optomotor responses below single photon level. *J Exp Biol.* 217: 4262–4268. DOI: 10.1242/jeb.112425.

Posted on 30 Aug 2023 — The copyright holder is the author/funder. All rights reserved. No reuse without permission. — https://doi.org/10.22541/au.169339743.30080820/v1 — This a preprint and has not been peer reviewed. Data may be preliminary.

Homberg U. 2015. Sky compass orientation in desert lousts–evidence from field and laboratory studies. *Front Behav Neurosci.* 9: 346. DOI: 10.3389/fnbeh.2015.00346

How MJ, Christy JH, Temple SE, Hemmi JM, Marshall NJ, Roberts NW. 2015. Target detection is enhanced by polarization vision in a fiddler crab.*Curr Biol.* 25: 3069–3073. DOI: 10.1016/j.cub.2015.09.073.

Hu ZL, Gu H, Hu J, He SL, Wang XQ, Liu XW, Jiao XN, Liu XF. 2018. Quantitative proteomics identify an association between extracellular matrix degradation and immunopathology of genotype VII Newcastle disease virus in the spleen in chickens. *J Proteomics* 181: 201–212. DOI: 10.1016/j.jprot.2018.04.019.

Ivanoff A, Waterman TH. 1958. Factors, mainly depth and wavelength, affecting the degree of underwater light polarization. *J Mar Res.*16: 283–307.

Jiang YL, Guo YY, Wu YQ, Duan Y, Miao J, Gong ZJ, Li T. 2012. Advances on response and perception mechanisms of insects to polarized light.*Acta Entomologica Sinica* 55: 226–232. DOI: 10.16380/j.kcxb.2012.02.014

Jonathan G, Atsuko A, Shah KK, Hirokawa JD, Magani PS, Gaby M. 2019. A neural circuit architecture for angular integration in Drosophila.*Nature* 7656: 101–106. DOI: 10.1038/nature22343.

Koyanagi M, Terakita A, Kubokawa K, Shichida, Y. 2002. Amphioxus homologs of Go-coupled rhodopsin and peropsin having 11-cis- and all-trans-retinals as their chromophores.*FEBS Lett.* 531: 525–528. DOI: 10.1016/S0014-5793(02)03616-5.

Kanehisa M, Goto S, Kawashima S, Okuno Y, Hattori M. 2004. The KEGG resource for deciphering the genome. *Nucleic Acids Res.* 32: D277–D280. DOI: 10.1093/nar/gkh063.

Kleinlogel S. 2006. Electrophysiological evidence for linear polarization sensitivity in the compound eyes of the stomatopod crustacean *Gonodactylus chiragra* . *J Expe Biol.* 209: 4262–4272. DOI: 10.1242/jeb.02499.

Kriska G, Csabai Z, Boda P, Malik P, Horvath G. 2006. Why do red and dark-coloured cars lure aquatic insects? The attraction of water insects to car paintwork explained by reflection-polarization signals.*Proc R Soc B Biol Sci.* 273: 1667–1671. DOI: 10.1098/rspb.2006.3500.

Levins R. 1968. Evolution in changing environments. Princeton: Princeton University Press.

Labhart T, Meyer EP. 1999. Detectors for polarized skylight in insects: a survey of ommatidial specializations in the dorsal rim area of the compound eye. *Microsc Res Techniq.* 47: 368–379. DOI: 10.1002/(SICI)1097-0029(19991215)47:6<368::AID-JEMT2>3.0.CO;2-Q.

Lamb TD, Pugh EN. 2006 Phototransduction, dark adaptation, and rhodopsin regeneration the proctor lecture. *Invest Ophth Vis Sci.* 47: 5137–5152. DOI: 10.1167/iovs.06-0849.

Luo YT, Sheng C, Qian ZY, Zhang HQ. 2006. The ultrastructure comparison of the light and dark adaptation of compound eyes in *Portunus tritubereulatus* . *Journal of Nanjing Normal University* 29: 82–85. (In Chinese)

Liu XQ, Bulgakov OV, Darrow KN, Pawlyk B, Adamian M, Liberman MC, Li TS. 2007. Usherin is required for maintenance of retinal photoreceptors and normal development of cochlear hair cells. *Proc Natl Acad Sci USA*104: 4413–4418. DOI: 10.1073/pnas.0610950104.

Leung YT, Fain GL, Matthews HR. 2007. Simultaneous measurement of current and calcium in the ultraviolet-sensitive cones of zebrafish.*J Physiol.* 579: 15–27. DOI: 10.1113/jphysiol.2006.120162.

Li H, Durbin R. 2009. Fast and accurate short read alignment with Burrows-Wheeler transform. *Bioinformatics* 25: 1754–1760. DOI: 10.1093/bioinformatics/btp324.

Lin-Jones J, Sohlberg L, Dose A, Breckler J,Hillman DW, Burnside B. 2009. Identification and localization of myosin superfamily members in fish retina and retinal pigmented epithelium. *J Comp Neurol.*5132: 209–223. DOI:10.1002/cne.21958.

Posted on 30 Aug 2023 — The copyright holder is the author/funder. All rights reserved. No reuse without permission. — https://doi.org/10.22541/au.169339743.30080820/v1 — This a preprint and has not been peer reviewed. Data may be preliminary.

Langmead B, Salzberg SL. 2012. Fast gapped-read alignment with Bowtie 2.*Nat Methods* 9: 357–359. DOI: 10.1038/nmeth.1923.

Liu ZY, Ding QW. 2015. Circularly polarized light identification mechanism analysis of mantis shrimp eyes. *Journal of Changchun University of Science and Technology* 38: 14–16, 21. (In Chinese)

Lelli A, Michel V, Boutet de Monvel J, Cortese M, Bosch-Grau M, Aghaie A, Perfettini I, Dupont T, Avan P, El-Amraoui A, Petit C. 2016. Class III myosins shape the auditory hair bundles by limiting microvilli and stereocilia growth. *J Cell Biol.* 212: 231–244. DOI: 10.1083/jcb.201509017.

Liu CH, Gong Z, Liang ZL, Liu ZX, Yang F, Sun YJ, Ma ML, Wang YJ, Ji CR, Wang YH, Wang MJ, Cui FA, Lin A, Zheng WS, He DF, Qu CX, Xiao P, Liu CY, Thomsen ARB, Cahill III TJ, Kahsai AW, Yi F, Xiao KH, Xue T, Zhou Z, Yu X, Sun JP. 2017. Arrestin-biased AT1R agonism induces acute catecholamine secretion through TRPC3 coupling. *Nat Commun.* 8: 14335. DOI: 10.1038/ncomms14335.

Lou F, Gao T, Cai S, Han Z. 2018. *De novo* assembly and annotation of the whole transcriptome of *Oratosquilla oratoria* . *Mar Genom.* 38: 17–20. DOI: 10.1016/j.margen.2017.08.003.

Lou FR, Han ZQ, Gao TX. 2019. Transcriptomic responses of two ecologically divergent populations of Japanese mantis shrimp*Oratosquilla oratoria* under thermal stress. *Animals* 9: 399. DOI: 10.3390/ani9070399.

Liu D, Pan YM, Li KY, Li DD, Li P, Gao ZM. 2020. Proteomics reveals the mechanism underlying the inhibition of *Phytophthora sojae* by propyl gallate. *J Agr Food Chem.* 68: 8151–8162. DOI: 10.1021/acs.jafc.0c02371.

Marshall NJ. 1988. A unique colour and polarization vision system in mantis shrimps. *Nature* 333: 557–560.

Marshall J, Land MF, King CA, Cronin TW. 1991. The compound eyes of mantis shrimps crustacea, hoplocarida, stomatopoda. I. Compound eye structure: the detection of polarized light. *Philos T Roy Soc B*334: 33–56. DOI: 10.1098/rstb.1991.0096.

McIntyre P, Caveney S. 1998. Superposition optics and the time of flight in onitine dung beetles. *J Comp Physiol A.* 183: 45–60. DOI: 10.1016/0300-9629(85)90036-2.

Marshall J, Cronin TW, Kleinlogel S. 2007. Stomatopod eye structure and function: a review. *Arthropod Struct Dev.* 36: 420–448. DOI: 10.1016/j.asd.2007.01.006.

Manor U, Disanza A, Grati M, Andrade L, Lin H, Di Fiore PP, Scita G, Kachar B. 2011. Regulation of stereocilia length by myosin XVa and whirlin depends on the actin-regulatory protein Eps8. *Curr Biol.*21: 167–172. DOI: 10.1016/j.cub.2010.12.046.

Miklos B, Adam E, Ramon H, Julia J, Miklos T, Krisztian K, Laszlo PB, Gyorgy K, Gabor H. 2012. No evidence for behavioral responses to circularly polarized light in four scarab beetle species with circularly polarizing exocuticle. *Physiol Behav.* 105: 1067–1075. DOI: 10.1016/j.physbeh.2011.11.020.

Marshall JN, Cronin TW. 2014. Polarized light and polarization vision in animal sciences. New York: Springer.

Nagata T, Koyanagi M, Tsukamoto H Terakita A. 2010. Identifcation and characterization of a protostome homologue of peropsin from a jumping spider. *J Comp Physiol A*.196: 51–59. DOI: 10.1007/s00359-009-0493-9.

Nagata T, Koyanagi M, Lucas R, Terakita A. 2018. An all-trans-retinal-binding opsin peropsin as a potential dark-active and light-inactivated G protein-coupled receptor. *Sci Rep.* 8: 3535. DOI:10.1038/s41598-018-21946-1.

Nityananda V, Tarawneh G, Henriksen S, Umeton D, Simmons A, Read JCA. 2018. A novel form of stereo vision in the praying mantis. *Curr Biol.* 28: 588–593. DOI: 10.1016/j.cub.2018.01.012.

Posted on 30 Aug 2023 — The copyright holder is the author/funder. All rights reserved. No reuse without permission. — https://doi.org/10.22541/au.169339743.30080820/v1 — This a preprint and has not been peer reviewed. Data may be preliminary.

Porter ML, Bok MJ, Robinson PR, Cronin TW. 2009. Molecular diversity of visual pigments in Stomatopoda Crustacea. *Visual Neurosci.* 26: 255–265. DOI: 10.1017/S0952523809090129.

Portera ML, Awataa H, Boka MJ, Cronina TW. 2020. Exceptional diversity of opsin expression patterns in *Neogonodactylus oerstedii* Stomatopoda retinas. *Proc Natl Acad Sci USA* 117: 8948–8957. DOI: 10.1073/pnas.1917303117.

Posner M, Kiss AJ, Skiba J, Drossman A, Dolinska MB, Hejtmancik JF, Sergeev YV. 2012. Functional validation of hydrophobic adaptation to physiological temperature in the small heat shock protein αA-crystallin.*PLoS ONE* 7: e34438. DOI: 10.1371/journal.pone.0034438.

Peña JF, Alié A, Richter DJ, Wang LY, Funayama N, Nichols SA. 2016. Conserved expression of vertebrate microvillar gene homologs in choanocytes of freshwater sponges. *EvoDevo* 7: 13. DOI 10.1186/s13227-016-0050-x.

Plubell DL, Wilmarth PA, Zhao YQ, Fenton AM, Minnier J, Reddy AP, Klimek J, Yang X, David LL, Pamir N. 2017. Extended multiplexing of tandem mass tags TMT labeling reveals age and high fat diet specific proteome changes in mouse epididymal adipose tissue. *Mol Cell Proteomics*16: 873–890. DOI: 10.1074/mcp.M116.065524.

Robertson BA, Hutto RL. 2006. A framework for understanding ecological traps and an evaluation of existing evidence. *Ecology* 87: 1075–1085. DOI: 10.1890/0012-9658(2006)87[1075:affuet]2.0.co;2.

Renninger SL, Gesemann M, Neuhauss SC. 2011. Cone arrestin confers cone vision of high temporal resolution in zebrafish larvae. *Eur J Neurosci.* 33: 658–667. DOI: 10.1111/j.1460-9568.2010.07574.x.

Robertson BA, Campbell DR, Durovich C, Hetterich I, Les J, Horváth G. 2017. The interface of ecological novelty and behavioral context in the formation of ecological traps.*Behav Ecol.* 28: 1166–1175. DOI:10.1093/beheco/arx081.

Shieh BH, Zhu MY. 1996. Regulation of the TRP Ca^{2+}channel by INAD in *Drosophila* photoreceptors. *Neuron* 16: 991–998. DOI: 10.1016/S0896-62730080122-1.

Satoh AK, Li BX, Xia H, Ready DF. 2008. Calcium-activated myosin V closes the *Drosophila pupil* . *Curr Biol.* 18: 951–955. DOI: 10.1016/j.cub.2008.05.046.

Salles FT, Merritt Jr RC, Manor U, Dougherty GW, Sousa AD, Moore JE, Yengo CM, Dosé AC, Kachar B. 2009. Myosin IIIa boosts elongation of stereocilia by transporting espin 1 to the plus ends of actin filaments.*Nat Cell Biol.* 11: 443–450. DOI: 10.1038/ncb1851.

Shashar N, Johnsen S, Lerner A, Sabbah S, Chiao CC, Mathger LM, Hanlon RT. 2011. Underwater linear polarization: physical limitations to biological functions. *Philos T Roy Soc B* 366: 649–54. DOI: 10.1098/rstb.2010.0190.

Schmeling F, Wakakuwa M, Tegtmeier J, Kinoshita M, Bockhorst T, Arikawa K, Homberg U. 2014. Opsin expression, physiological characterization and identification of photoreceptor cells in the dorsal rim area and main retina of the desert locust, *Schistocerca gregaria* . *J Exp Biol.* 217: 3557–3568. DOI:10.1242/jeb.108514.

Simão FA, Waterhouse RM, Ioannidis P, Kriventseva EV, Zdobnov EM. 2015. BUSCO: assessing genome assembly and annotation completeness with single-copy orthologs.*Bioinformatics* 19: 3210–3212. DOI: 10.1093/bioinformatics/btv351.

Sakurai K, Vinberg F, Wang T, Chen J, Kefalov VJ. 2016. The Na^{+}/Ca^{2+}, K^{+}exchanger 2 modulates mammalian cone phototransduction. *Sci Rep.*6: 32521. DOI: 10.1038/srep32521.

Shen M, Zhang N, Zheng SD, Zhang WB, Zhang HM, Lu ZK, Su Q, Sun YJ, Ye KQ, Li XD. 2016. Calmodulin in complex with the first IQ motif of myosin-5a functions as an intact calcium sensor. *P Natl Acad Sci USA* 113: E5812–E5820. DOI: 10.1073/pnas.1607702113.

Posted on 30 Aug 2023 — The copyright holder is the author/funder. All rights reserved. No reuse without permission. — https://doi.org/10.22541/au.169339743.30080820/v1 — This a preprint and has not been peer reviewed. Data may be preliminary.

Thoen HH, How MJ, Chiou TH, Marshall J. 2014. A different form of color vision in mantis shrimp. *Science* 343: 411–413. DOI: 10.1126/science.1245824.

Templin RM. 2017. Circular polarization vision in stomatopod crustaceans. Queensland: The university of Queensland.

von Philipsborn A, Labhart T. 1990. A behavioural study of polarization vision in the fly, *Musca domestica* . *J Comp Physiol.* 167: 737–743. DOI: 10.1007/BF00189764.

Vinberg F, Wang T, De Maria A, Zhao H, Bassnett S, Chen J, Kefalov VJ. 2017. The Na^+/Ca^{2+}, K^+exchanger NCKX4 is required for efficient cone-mediated vision.*Elife* 6. DOI: 10.7554/eLife.24550.

Wilden U, Hall SW, Kühn H. 1986. Phosphodiesterase activation by photoexcited rhodopsin is quenched when rhodopsin is phosphorylated and binds the intrinsic 48-kDa protein of rod outer segments. *Proc Natl Acad Sci USA* 83: 1174–1178. DOI: 10.1073/pnas.83.5.1174.

Witherington BE 1997. The problem of photopollution for sea turtles and other nocturnal animals. In: Clemmons JR, Bucholz R, editors. Behavioral approaches to conservation in the wild. Cambridge: Cambridge University press. P. 303–328

Wu J, An Y, Pu H, Shan Y, Ren XQ, An MR, Wang QS, Wei SC, Ji JG. 2010. Enrichment of serum low-molecular-weight proteins using C_{18} absorbent under urea/dithiothreitol denatured environment. *Anal Biochem.* 398: 34–44. DOI: 10.1016/j.ab.2009.10.047.

Wang W, Chu JK, Cui Y, Zhi W, Chen C. 2013. Modeling of atmospheric polarization pattern based on vector radiative transfer. *Chinese Journal of Lasers* 40: 220–226. (In Chinese)

Yuan F, Bernard GD, Le J, Briscoe AD. 2010. Contrasting modes of evolution of the visual pigments in *Heliconius butterflies* .*Mol Biol Evol.* 27: 2392–2405. DOI: 10.1093/molbev/msq124.

Zhao W, Yang QB, Chen X, Chen MQ, Wen WG. 2019. A review of research on the biological properties and reproductive biology of some mantis shrimps. *Maine Sciences* 43: 105–114. (In Chinese)

Zang JJ, Neuhauss SCF. 2021. Biochemistry and physiology of zebrafish photoreceptors. *Pflug Arch Eur J Phy.*473: 1569–1585. DOI: 10.1007/s00424-021-02528-z.

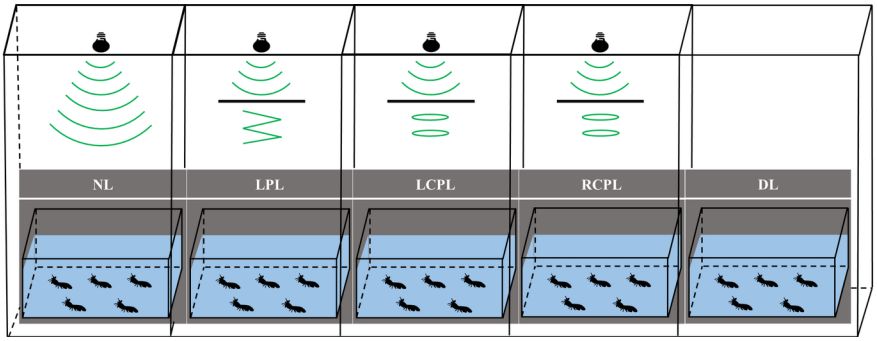

Posted on 30 Aug 2023 — The copyright holder is the author/funder. All rights reserved. No reuse without permission. — https://doi.org/10.22541/au.169339743.30080820/v1 — This a preprint and has not been peer reviewed. Data may be preliminary.

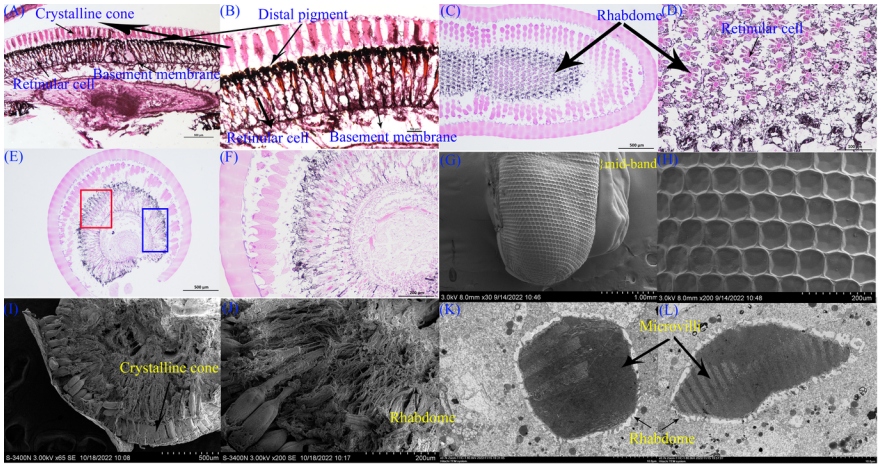

Posted on 30 Aug 2023 — The copyright holder is the author/funder. All rights reserved. No reuse without permission. — https://doi.org/10.22541/au.169339743.30080820/v1 — This a preprint and has not been peer reviewed. Data may be preliminary.

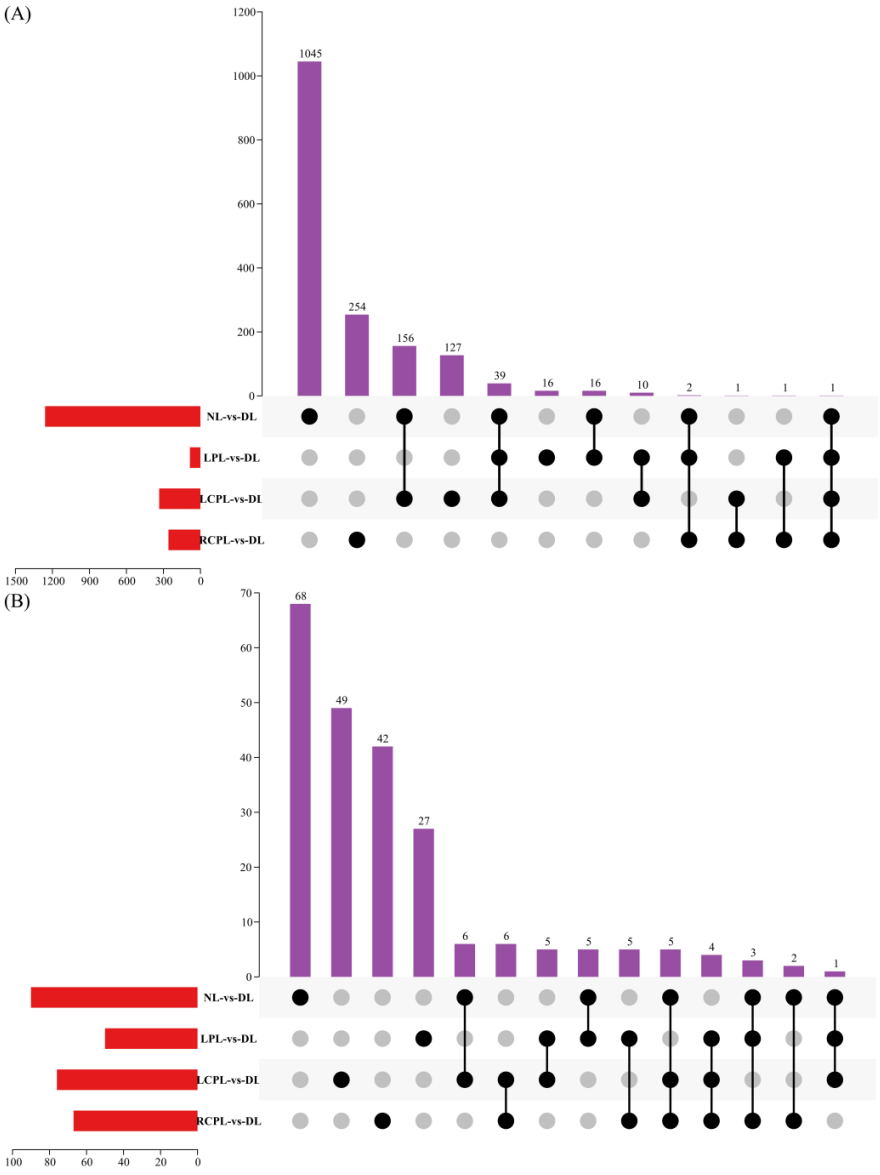

Posted on 30 Aug 2023 — The copyright holder is the author/funder. All rights reserved. No reuse without permission. — https://doi.org/10.22541/au.169339743.30080820/v1 — This a preprint and has not been peer reviewed. Data may be preliminary.

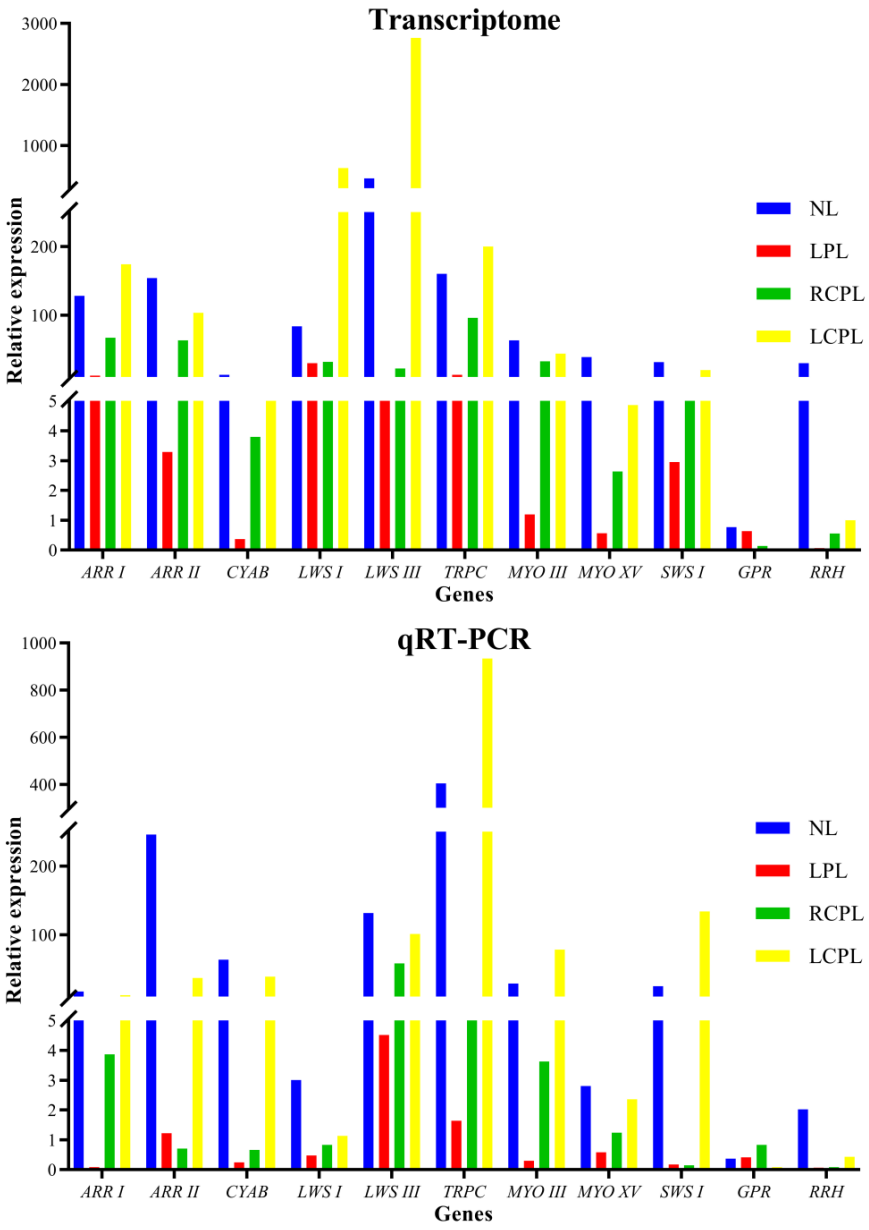

Posted on 30 Aug 2023 — The copyright holder is the author/funder. All rights reserved. No reuse without permission. — https://doi.org/10.22541/au.169339743.30080820/v1 — This a preprint and has not been peer reviewed. Data may be preliminary.

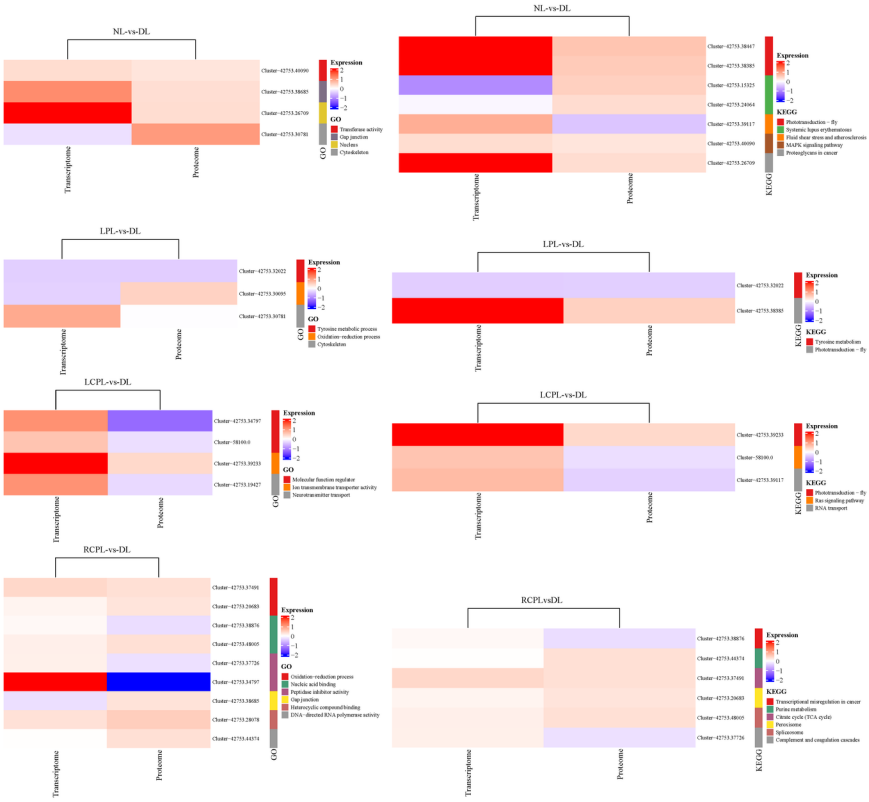

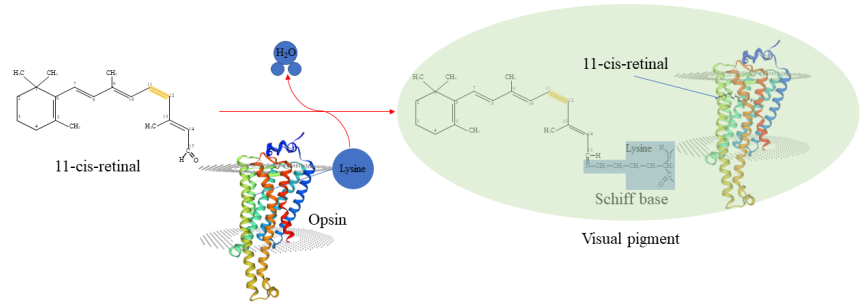

Posted on 30 Aug 2023 — The copyright holder is the author/funder. All rights reserved. No reuse without permission. — https://doi.org/10.22541/au.169339743.30080820/v1 — This a preprint and has not been peer reviewed. Data may be preliminary.

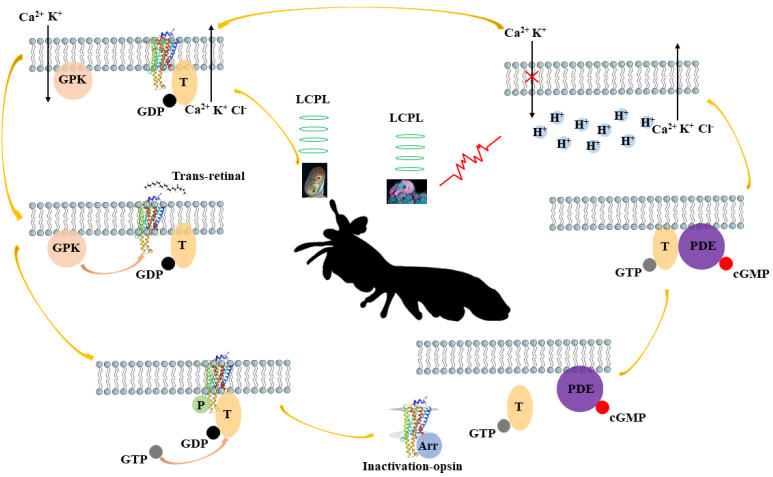

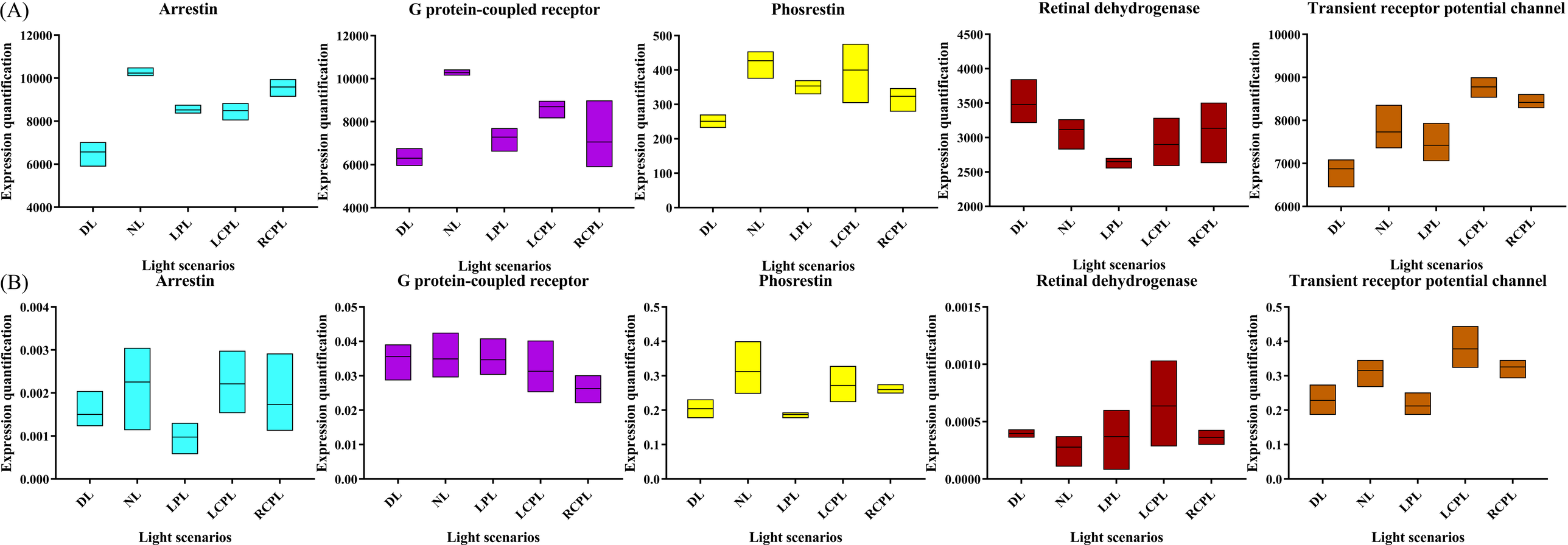
(A)
Arrestin
G protein-coupled receptor
Phosrestin
Retinal dehydrogenase
Transient receptor potential channel
Expression quantification
Light scenarios
DL
NL
LPL
LCPL
RCPL
(B)
Arrestin
G protein-coupled receptor
Phosrestin
Retinal dehydrogenase
Transient receptor potential channel
Expression quantification
Light scenarios
DL
NL
LPL
LCPL
RCPL